2022-12-01

Fabrication And Characterization Of Germanium Functionalized Porous Nickel Oxide Electrodes For Application In Supercapacitors

Cristina Gonzalez
University of Texas at El Paso

FABRICATION AND CHARACTERIZATION OF GERMANIUM FUNCTIONALIZED POROUS NICKEL OXIDE ELECTRODES FOR APPLICATION IN SUPERCAPACITORS

CRISTINA GONZALEZ

Master's Program in Mechanical Engineering

APPROVED:

Chintalapalle Ramana, Ph.D., Chair

Ahmed El-Gendy, Ph.D.

Das Debabrata, Ph.D.

Stephen L. Crites, Jr., Ph.D.
Dean of the Graduate School

FABRICATION AND CHARACTERIZATION OF GERMANIUM FUNCTIONALIZED POROUS NICKEL OXIDE ELECTRODES FOR APPLICATION IN SUPERCAPACITORS

By

CRISTINA GONZALEZ

THESIS

Presented to the Faculty of the Graduate School of

The University of Texas at El Paso

in Partial Fulfillment

of the Requirements

for the Degree of

MASTER OF SCIENCE

Department of Aerospace and Mechanical Engineering

THE UNIVERSITY OF TEXAS AT EL PASO

December 2022

ACKNOWLEDGEMENT

My most sincere appreciation goes to Professor C.V Ramana, my advisor, for his guidance, support, time and understanding in helping me succeed in my studies. He always motivated me to learn and do better in academic and research work. Also, I would like to thank Dr. Balwant Kr Singh for supervising and assisting me throughout my research. Without his guidance, knowledge and support this thesis would not have been possible. I am also thankful to my research committee members Prof. Ahmed El-Gendy and Dr. Debabrata Das for fruitful discussion and appreciation. To conclude, I am grateful to my research team (CRM) for their support and advice.

ABSTRACT

Limited fossil fuel, increasing population, pollution, and climate change are motivating society to use renewable and clean energy techniques. However, the intermittent nature of renewable sources hinders their continuous availability and use. Energy storage devices such as supercapacitors and batteries are essential for sustainable development but their high cost limits its bulk use. The cost of energy storage devices mainly depends on materials, synthesis process and device fabrication. Therefore, low cost 3-D mesoporous nickel germanium fictionalize nickel oxides electrode materials has been developed by using facile fabrication techniques for supercapacitor application. 3-D mesoporous nickel provides the high surface area and enhances the ionic conductivity, germanium functionalization improves the electrical conductivity and reduces the charge transfer resistance of nickel oxides. Germanium fictionalization demonstrates the improvement in specific capacitance of nickel oxides by more than twice. The asymmetric supercapacitor shows the specific capacitance of 36 $mFcm^{-2}$, energy density of 2.5 $\mu Whcm^{-2}$, and power density of 0.67 $mWcm^{-2}$. The digital watch powered by germanium functionalized nickel oxides and activated carbon-based asymmetric supercapacitor shows practical application of the device.

TABLE OF CONTENTS

Page

LIST OF TABLES

LIST OF FIGURES

CHAPTER 1: INTRODUCTION

1.1 Research motivation

In 2021 the energy consumption in the United States consisted of 36% petroleum , 32% Natural Gas, 10% coal, 8.1% nuclear, and only 12 % from renewable energy sources[1]. More than three- fourths of the energy comes from fossil fuels. There is strong evidence that demonstrates the effect the use of fossil fuels for transportation, electricity and industrial processes has had on the environment. Such as, climate change, air pollution, global warming, and the depletion of the ozone layer. The burning of fossil fuels such as coal, oil and gas has led to an increase of concentration of carbon dioxide and other greenhouse gasses in the atmosphere. Naturally, the greenhouse gasses are part of the earth's atmosphere. It helps keep the earth warm by trapping heat from the sun. Without the greenhouse effect, the earth would be colder. By increasing the carbon dioxide as well as other greenhouse gasses in the atmosphere, more heat gets trapped, making the temperature rise. It is projected that if continued dependence on fossil fuels the global surface temperature increase will likely exceed 1.5 degrees celsius [2]. The rise in temperature has caused changes to the ecological environment because of sea-level rise, glacier melting, and ocean acidification[3].

1.2 Background

The power density vs energy density mostly known as Ragone plot is shown in Figure 1.1. It compares the current energy storage devices based on their energy and power densities. It can be seen that capacitors have high power density but low energy density. This means that it is able to discharge and charge at a faster rate. On the other hand, batteries and fuel cells have high

energy density but low power density. This means they are able to store more energy but take longer to charge and discharge. Supercapacitors are in between capacitors and batteries. Its energy storage is better than a capacitor but not as good as a battery. As for its power density it is better than a battery but not as high as a capacitor. Future energy storage systems must provide high energy density as well as high power density.

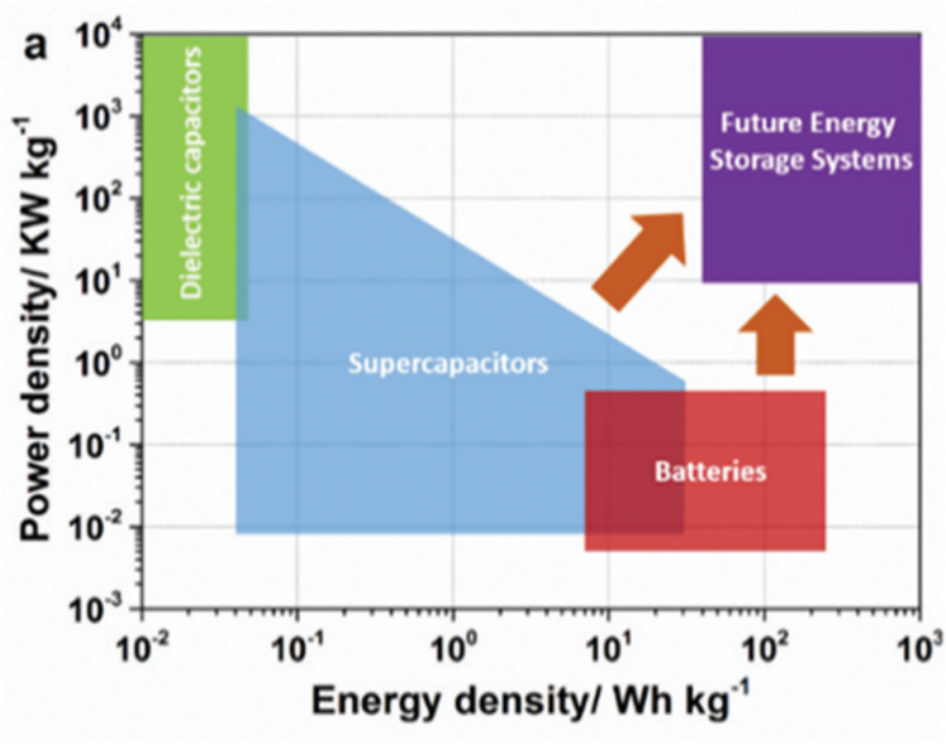

Figure 1.1: Energy density vs power density for energy devices [4]

As stated above batteries provide high energy storage and are used in most applications. Yet, they are lacking in other characteristics. For that reason, supercapacitors are viewed as alternatives to conventional batteries. It is essential for an energy storage device to have both high energy and power densities. Not only that but, long life cycles, high durability, fast charging and properties that are safe to the environment. The table below shows differentiation

of characteristics of batteries and supercapacitors. It can be seen that supercapacitors are superior in cycle life, power density, charge/ discharge time, and durability. The life cycle of a battery is relatively low in comparison to supercapacitors. It is important to have long life cycles because they are subjected to repeated charge and recharge cycles. As for the charge and discharge time, supercapacitors are by far superior to batteries. Its charging time is between .3 to 30 seconds and its discharge is the same. Batteries have a charging time between one hour to five hours and a discharge time of .3 to 3 hours. That said, supercapacitors show quality characteristics and can be improved to ultimately replace batteries.

Table 1.1: Comparison of batteries and supercapacitors

Characteristics	Li-ion Batteries	Supercapacitors	Ref.
Cycle life	500-3000	10^4-10^6	[5,6,7]
Power Density (kW/kg)	.5-1	10-13	[5,8]
Energy Density (Wh/kg)	70-200	3-180	[5,7]
Discharge time (s)	1,080-10,800	.3-30	[5,6]
Charge time (s)	3,600-18,000	.3-30	[5,6]
Durability (Years)	10-20	20	[5]
Cell Voltage (V)	2.3 - 2.8	2.5 - 4.2	[7]

The main challenges for supercapacitors to overcome are low energy density and cost. There has been much done to improve the energy density of supercapacitors and broaden their application. Most of the research has been made on advanced electrode materials to increase the cell voltage as well as the capacitance. Since capacitance and voltage are both proportional to energy density, if either are increased it will increase the energy density. This can be done by developing hybrid or asymmetric supercapacitors, and by using new electrolytes. The

development of electrolytes can widen the potential window and increase the cell voltage. It is more efficient to increase the cell voltage since the energy density is proportional to the square of the cell voltage[9]. It should be noted that interactions between each component must be considered when improving the supercapacitor.

1.3 Objective and organization of thesis

The objective of this research is to fabricate Ge-NiO electrode materials by electrodeposition.It will be optimized with different electrodeposition times to see which deposition time shows better results.To see which one shows better results, the material properties will be studied with the use of physical and chemical characterization. For physical characterization methods such as X-ray diffraction, Scanning electron microscopy and EDS will be used. As for the electrochemical characterization, cyclic voltammetry, galvanic charge/ discharge will be used. From the study of the characterization Ge-NiO-4 shows a better performance and will be used for the asymmetric supercapacitor. The asymmetric supercapacitor will be tested with electrochemical characterization. Lastly, the asymmetric supercapacitor will be tested to show its performance.

1.4 Literature

1.4.1 Types of supercapacitors

There has been a lot of research done in order to improve or replace current methods to store energy. Conventional energy sources such as wind, solar etc. have their limitations. For example, solar energy can not be produced at night and wind energy can not be produced if there is no wind. With that being said, supercapacitors are widely used as energy storage devices due

to their energy storage capabilities. They are classified as electrochemical double layer, pseudocapacitors and hybrid supercapacitors. In electrochemical double layer energy is stored through the adsorption and desorption of ions at the electrode/electrolyte interface. Pseudocapacitors store energy through surface faradic redox reactions[10].

1.4.1.1 Electric double layer capacitors

The first electric double layer model proposed is shown in Figure 1.2 (a). Helmholtz stated that two layers of charge formed at the electrode and the electrolyte are separated by a small distance, H[11].In Figure 1.2 (b) shows the Helmholtz model modified by Gouy in 1910 and Chapman in 1913. Instead of having the ions close to the electrode surface, the ions are distributed in the diffuse layer. This model takes into account that ions are moving in the electrolyte and are driven by the influence of the diffusion and electrostatic forces[12]. Later in 1924, Stern combined the previous models to form the Gouy-Chapman-Stern model. The Stern layer is similar to the Helmholtz model. It is described as a compact layer of immobile ions that are absorbed at the surface of the electrode[12]. It also has the diffuse layer shown in the Gouy-Chapman model. As stated before, the ions are mobile in the diffuse layer. The principles of the Gouy-Chapman-Stern model are mostly used in the development of electrochemical double layer capacitors.

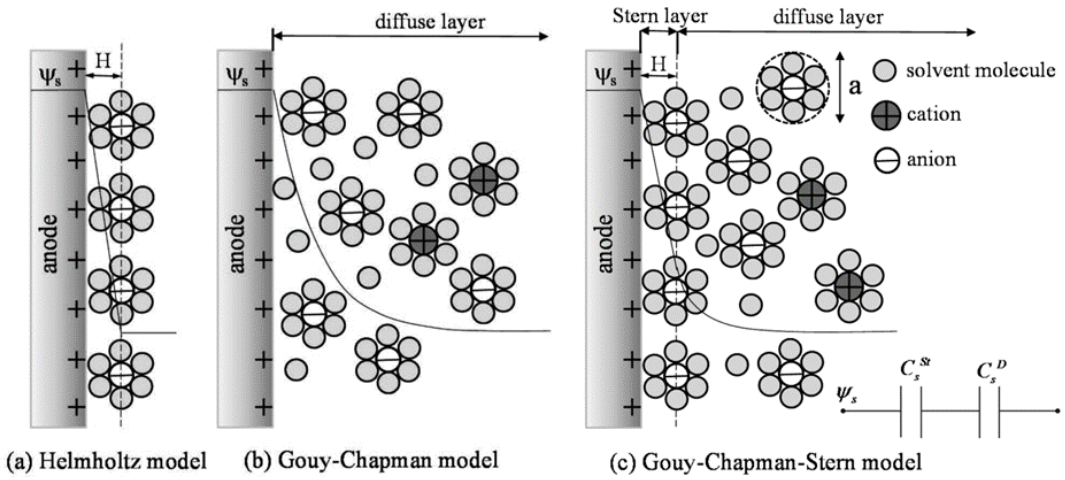

Figure 1.2: Schematic representation of electric double layer capacitor (a) Helmholtz model, (b) Gouy-Chapman model, and (c) Gouy-Chapman-Stern model [12].

A double layer capacitor is composed of an electrolyte, two carbon based electrodes, and a separator. The energy storage process takes place between the electrode and the electrolyte where energy is stored by ion absorption. During the charging process voltage is applied and both the positive electrode and negative electrode get charged. The positive ions from the electrolyte are attracted to the negative electrode and the negative ions are attracted to the positive electrode. An electric double layer is formed in the two electrodes. For the discharge a load is applied and the electrodes lose their charge and flow into the external circuit. The ions from the electrolyte are no longer attracted to the electrodes and get scattered again in the electrolyte section as shown in Figure 1.3.

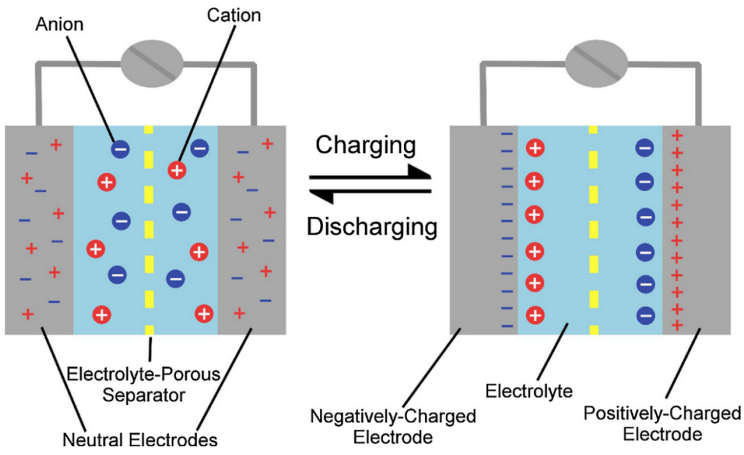

Figure 1.3 Schematic of charge/discharge in EDLC [13]

1.4.1.2 Pseudocapacitors

In the previous section EDLC were discussed. Its energy storing process takes place between the surface of the electrode and the electrolyte. For that reason its performance is dependent on the surface area as well as the type of electrolyte. In order to increase its surface area a porous electrode is created. Yet, even with a porous electrode its performance is not enough to replace batteries. For that reason other materials and storage mechanisms are being studied.

Unlike EDLC's, pseudocapacitors store energy through faradaic reactions at the electrode surface. The different Faradaic reactions are underpotential deposition, redox reduction and intercalation. Figure 1.4 shows a schematic of the underpotential deposition, redox, and intercalation reactions. During the underpotential deposition, lead ions from the electrolyte form a monolayer on the surface of the gold electrode. In other words, adsorption and desorption of atoms from the electrolyte on a metal surface[14]. In redox reaction takes place near or at the surface of the electrode.During charging and discharging no chemical changes happen to the

surface of the electrode because of reversible redox reactions. For example, from Figure 1.4 (b) RuO gets reduced during charging and when discharging the ions go back to the electrolyte and back to its original form. Lastly, in intercalation the ions from the electrolyte intercalate in the layers of the material[13].

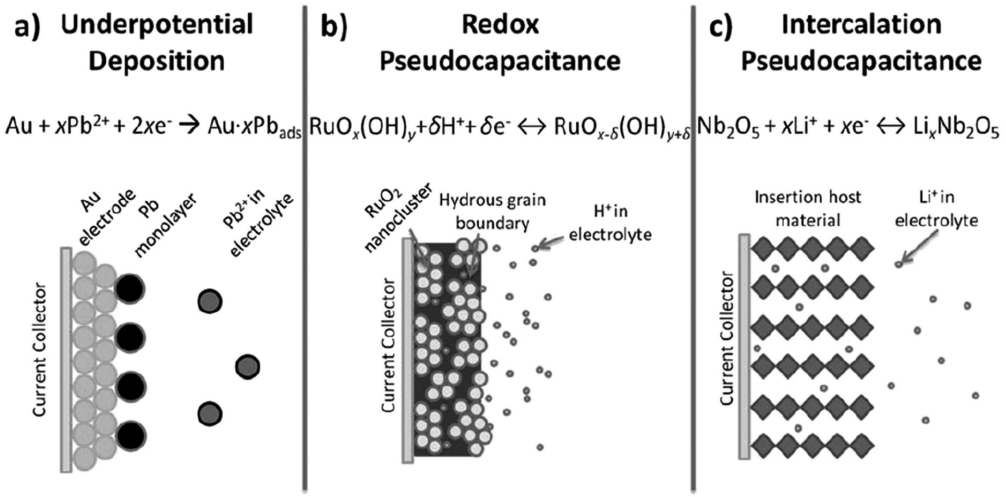

Figure 1.4 : pseudocapacitor reactions (a) underpotential deposition (b) redox (c) intercalation [13]

1.4.1.3 Hybrid

Hybrid supercapacitors have more enhanced characteristics due to the combination of energy storage mechanisms. They may be asymmetric as well as symmetric based on the materials of the electrodes. Overall supercapacitors exhibit greater power density, but lower energy density when compared to batteries. To improve its performance, many researchers are focusing on the development of materials that show superior energy density in close approximation to that of batteries. This without altering the characteristics of high power density along with long cycling life[15].

Hybrid supercapacitors are made of different electrode materials. This means the electrodes store energy in a combination of EDLC and pseudocapacitor principles. Having said that, hybrid capacitors use three types of electrodes: composite, battery type, and asymmetric[16]. For composite, carbon based materials are integrated with a conducting polymer or a metal oxide.The carbon material performs the role of the EDLC and metal oxides or polymer of a pseudocapacitive reaction. With that carbon based material will provide a high surface area while the pseudocapacitive material can increase the capacitance[17]. The battery type is composed of a supercapacitor electrode and a battery electrode. This helps by combining the characteristics of batteries with that of supercapacitors. Batteries exhibit high energy density while supercapacitors exhibit high power density, cycle life, and recharge time. Lastly, asymmetry has a EDLC electrode and a pseudocapacitive electrode. Generally, the negative electrode is carbon based and the positive electrode is of a metal oxide or a conducting polymer. This attains to higher energy and power densities compared to EDLC and better cycling than symmetric pseudocapacitors[17].

1.4.2 Materials for supercapacitors

As stated before, the material of the electrode is important because it plays an important role in the performance of the supercapacitor. Electrical double layer capacitors are composed of carbon materials such as activated carbon, carbon nanotubes, graphene to name a few. Pseudocapacitors consist of metal oxides and conducting polymers. Hybrid supercapacitors will vary depending on the type of mechanism. For a symmetric hybrid , the anode and cathode will consist of a pseudocapacitance material. An asymmetric hybrid will consist of a pseudocapacitor as the anode and a double layer capacitor as the cathode. That is, a metal oxide or conducting polymer and a carbon material.

1.4.2.1 Carbon

1.4.2.1.1 Activated Carbon

Activated carbon is an essential form of carbon because its properties allow its use in various applications[18]. Properties such as high surface area, good electrical performance, variable pore size, chemical stability, and low cost make it an interesting choice [18,19]. Activated carbon was obtained by burning carbon materials such as coal and petroleum coke. However, in the last few years research has been made to get activated carbon with renewable materials. Table 1.2 shows a couple of raw materials used in research for the preparation of activated carbon. When looking for renewable carbon materials , researchers look for high carbon content and at the same time have a tunable morphology of the obtained products to be utilized in supercapacitor application[20].

Table 1.2: Activated Carbon from renewable materials

Precursors	Surface area (m2 g-1)	Reference
Petroleum coke	2532	[20]
Phenol-formaldehyde resins	2445	[20]
Coconut shells	1194, 1416, 1440	[20]
Waste coffee beans	1019	[20]
Metal-organic framework	2222	[20]
Tofu	2960	[20]
Birch sawdust	3300	[20]
Oil palm shells	2139	[20]
Tree bark	1018	[20]

Wheat straw	2316	[20]
Bamboo cellulose fiber	2366	[20]
Walnut shells	1197	[20]
Cabbage leaves	3102	[20]
Fish gill	2082	[20]
Pumpkin	2968	[20]
Starch	1510	[20]
Rice husk	1390,1890	[21]
Apricot shell	2335	[21]
Firwood	1130	[21]
Potato starch	2340	[21]
Banana	1414	[22]
Cauliflower	2604	[22]
Garlic Skin	2818	[22]
Dragon fruit peel	2667	[22]
Orange Peel	2521	[22]
Human hair	1306	[22]

Aside from selecting a material it is also important to take into consideration the process of synthesis. The first step in the synthesis process is carbonization. In which the non-carbon species are eliminated from the biomasses by thermal decomposition, resulting in the enrichment of carbon content in the carbonaceous material[18]. Figure 1.5 shows a 3- dimensional schematic of activated carbon derived from coconut fibers. It can be seen that in the carbonization process the porosity is low and will later be improved. Then the burned material called char would then be chemically and physically treated. The physical activation is done at high temperatures between 700-1200 degrees celsius, and occurs in assorted oxidizing atmospheres[19,22]. Such as

air, oxygen, carbon dioxide, and water vapor and treated for a period of time to acquire the final product[22]. The chemical activation is done at lower temperatures between 400 -700 degrees celsius [19]. Some of the activating agents commonly used are H_2SO_4, HNO_3, H_3BO_3,$ZnCl_2$, H_3PO_4, NaOH and KOH [18, 22]. As shown in the figure below, with the physical and chemical activation the porosity is improved.

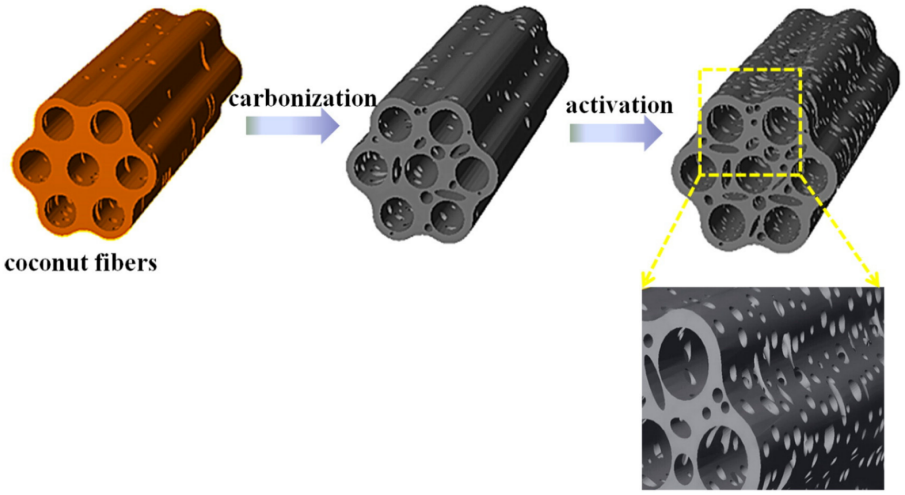

Figure 1.5 :Porous activated carbon [23]

As mentioned in earlier sections Electrical double layer capacitor is composed of two electrodes made of carbon material. Activated carbon can be produced while being environmentally friendly, low cost, and the materials are available in abundance. Yet, there are still challenges in the development of activated carbon through biomass for supercapacitors[22].

1.4.2.1.2 Carbon Nanotubes (CNT)

In 1991, Ijima discovered carbon nanotubes containing more than one graphitic layer and an inner diameter of 4nm. In 1993, Bethune et al. and Ijima et al. reported the development of

single- walled nanotubes [18]. Having said that, carbon nanotubes are categorized based on the tube structure and shape. One is single walled carbon nanotubes (SWCNT) and the other one is multi walled carbon nanotubes(MWCNT) . A SWCNT is a graphite sheet curled into a cylindrical form. The MWCNT contains many concentric single walled nanotubes with different diameters[19]. Carbon nanotubes have the capability to perform in multiple fields. Its pore structure, electrical characteristics, thermal, and mechanical properties makes them a potential performer in fields such as supercapacitors, fuel cells, high strength composites, biomedical and chemical[18 ,24]. It can be seen from Figure 1.6, that CNT's are considered for supercapacitors due to the surface area and electrical conductivity.

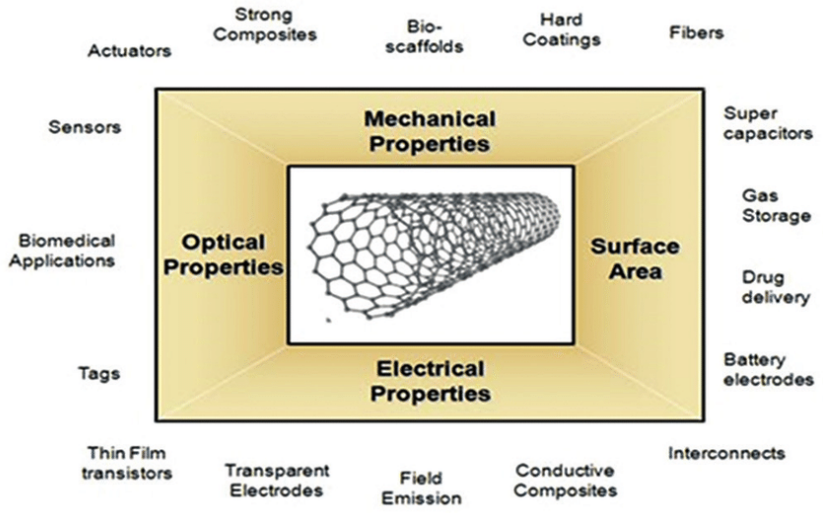

Figure 1.6 : Carbon nanotubes properties and its application [25]

1.4.2.1.3 Graphene

Graphene is a one atom thick sheet made of sp2 bonded carbon atoms in a honeycomb crystal lattice[21]. As shown in Figure 1.7 , graphene is obtained from the graphite which contains many layers of graphene[26].That said, graphene has potential in energy storage devices because of its high cyclic life, excellent thermal and chemical properties[19].

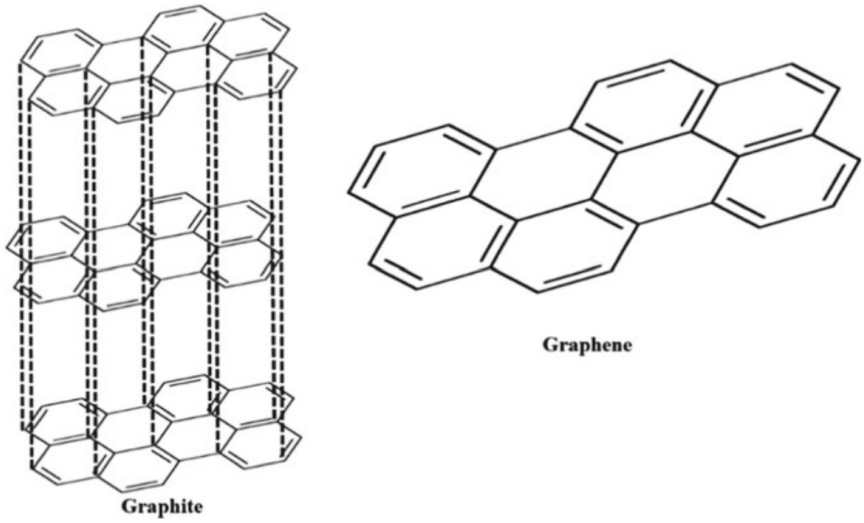

Figure 1.7: Schematic of graphite and graphene honeycomb lattice [26]

Carbon is one of the most abundant elements on earth. And so, carbon has many physical forms. The most known are graphite and diamond. It wasn't until 1960, that the characteristic of graphite was revealed to consist of layers [27]. Figure 1.8 shows carbon materials in other dimensions. For example, the one on the left is zero dimension fullerenes, the second one is one dimension nanotubes and the third one is three dimensional graphite. It can be seen that graphite consists of many layers like stated before. Therefore, one layer of the graphite is known as graphene. According to Mouras et al. (1987), the term “graphene” first appeared in 1987. It depicted a single sheet of graphite, which is the main building block of materials such as graphite, fullerene, and carbon nanotubes[27].

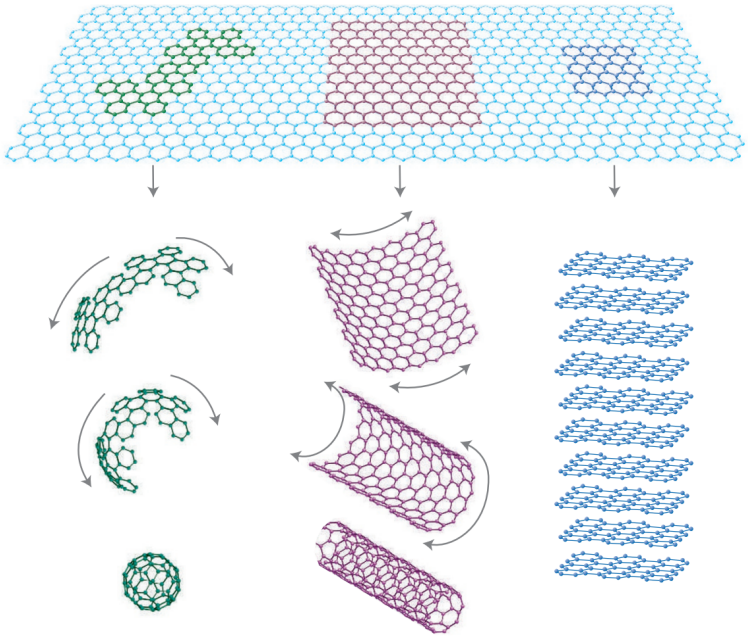

Figure 1.8 : Graphene in other dimensionalities [28]

The synthesis of graphene is based on physical and chemical methods. Some common graphene synthesis methods are mechanical exfoliation, liquid phase exfoliation, oxidation-reduction, chemical vapor deposition, and epitaxial growth on silicon carbide. The mechanical exfoliation was developed in 1990 by Kurz and co workers. It is a single step and simple procedure but time consuming and expensive. [26]. In order to improve this method another approach was taken. Chen and his teammates discovered a method via a three roll mill. The other process is the liquid phase exfoliation. This method converts graphite into monolayers in liquid phase via ultrasonication[26]. Next are the two most common synthesis of graphene. In oxidation-reduction, oxidation of graphite is followed by chemical reduction. This offers low cost mass production of reduced graphene oxide (rGO), which can directly be used as EDLC electrode materials[29] . Lastly, chemical vapor deposition deposits carbon atoms on growth substrates via chemical reactions[26].

Graphene based supercapacitors were reported with specific capacitance of 75 F g-1 and energy density of 31.9 W h kg-1 with ionic liquid electrolytes. As for aqueous and organic electrolyte the specific capacitance of 135 F g-1 and 99 F g1, respectively. [21]. Yet, through doping the electrochemical properties of graphene have been improved. For example, Jeong et al. synthesized N-doped graphene through a simple plasma process and it is found to exhibit a specific capacitance of 280 F g−1 , which is 4 times higher than that of the corresponding undoped graphene[29].

1.4.2.2 Metal Oxides

Transition metals are located in the periodic table from groups three to eleven. These transition metals have partially filled d-subshells or ionizes to give cations with an incomplete d orbital[18]. Thus, in order for a metal oxide to be suitable for supercapacitor application they must satisfy certain conditions. One is that they should be electronically conductive. Second, the metal can exist in two or more oxidation states with no phase changes involving irreversible modifications of a 3D structure. Lastly, the protons can intercalate freely, into the oxide lattice on reduction and out in oxidation. [29]. Several transition metals have shown high specific capacitance, good electrical conductivity, reversible charge -discharge properties, and excellent power densities[30]. Yet, various transition metal oxides have demonstrated to be harmful to the environment and costly. For that reason the metal oxides that have been mostly reviewed are ruthenium oxide, manganese oxide, cobalt oxide, and nickel oxides. Apart from ruthenium oxide, the materials mentioned have been considered for supercapacitors due to its excellent pseudocapacitive behavior, availability, environment safe and cost effectiveness[30]. However, one main setback is its poor conductivity which is not good in supercapacitor performance. For

that reason composites of metal oxides are being developed to improve the performance. Furthermore, preparation of metal oxides involves synthesis. It is a very important step because the preparation method will affect its performance. Table 1.3 shows some preparation methods for metal oxides.

Table 1.3: Preparation methods for metal oxides in supercapacitors

Preparation Method	**Description of method**	**Metal Oxide Example**	**Ref.**
High temperature solid state	Solid precursors are mixed intimately and then reacted at a high temperature	Co_3O_4	[31]
Hydrothermal	The precursor is dissolved in deionized water or organic solvent and then heated in an airtight reaction autoclave. This produces a crystalline product.	MnO_2 NiO	[31]
Templating	Organic materials are usually prepared to form a template with a distinct morphology and then the metal sample grows at their surface.The target product is obtained by removing the organic template.	Hollow structured Co_3O_4 MnO_2	[31]
Sol-gel	The precursors form a sol by undergoing hydrolysis and condensation reactions. The sol slowly polymerizes to form a gel, and then the gel generates nanomaterial	MnO_2 nanowire arrays $NiO/NiCo_2O_4/Co_3O_4$ composite	[31]

	by drying and curing.		
Electrodeposition method	Electrochemical principles are used to deposit metal ions and insoluble particles in suspension to obtain the desired product on the cathode surface.	RuO_2 MnO_2	[31]
Chemical Vapor Deposition (CVD)	Compounds or gasses generate a nonvolatile solid membrane layer or nanomaterial on a suitable substrate surface.	ZnO TiO_2	[31]
Chemical precipitation	In this method, a chemical reaction between different components in solution is used to form an insoluble product. When the precipitation reagent solution is added dropwise to an inorganic solution, the product is formed rapidly and uniformly dispersed.	$Ni(OH)_2$ SnO_2	[31]

1.4.2.2.1 Ruthenium Oxide

Ruthenium is a metal element that is a member of the platinum group. Even Though it is an uncommon metal, it is the cheapest among the platinum group, but costly among other transition metals. Moreover, ruthenium can exist in three oxidation states +2,+3 and +4 within a voltage window of 1.2 V[29,31]. From all the metal oxides ruthenium oxide is the leading material due to its advantages. For example, it has the highest specific capacitance out of all the pseudocapacitance materials, between 200 up to 1200 Fg-1. Factors such as specific surface area,

combined water, degree of particle crystallinity, particle size, electrode architecture and electrolyte have an effect on specific capacitance[29, 31].

Although ruthenium oxide has shown great theoretical capacitance, its high cost has been a major drawback. For that reason many researchers have attempted to reduce ruthenium usage with the use of composite materials. Two methods are being used. The first one is to deposit RuO_2 on other low cost material. The second one is to dope RuO_2 with base metal oxides[31]. In addition, Ruthenium dioxide exists in two structures, anhydrous and hydrous forms[32]. One which contains water molecules and the other one does not. It can be seen in Table 1.4 that RuO_2 and $RuO_2 \cdot xH_2O$ is deposited into low cost materials like carbon nanotubes, multi walled carbon nanotubes, activated carbon, conducting polymers,and graphene. Also, into metals like tin and titanium.

Table 1.4: Ruthenium Dioxide performance with low-cost materials

Ru- based material	**Electrode material**	**Current density**	**Specific capacitance**	**Electrolyte**	**Ref.**
RuO_2	RuO_2	-	788	.5 M H_2SO_4	[33]
RuO_2	RuO_2	-	650	.5 M H_2SO_4	[33]
RuO_2	RuO_2/CNT	.5	966.8	1 M H_2SO_4	[33]
RuO_2	RuO_2/CNT	-	1170	.5 M H_2SO_4	[33]
RuO_2	RuO_2/MWCNT	-	457.63	1 M H_2SO_4	[33]
RuO_2	RuO_2/C	.5	879.1	1 M H_2SO_4	[33]
RuO_2	RuO_2/C	.05	537.7	1 M H_2SO_4	[33]
RuO_2	RuO_2/rGO	.5	1099.6	1 M H_2SO_4	[33]

RuO_2	RuO_2/PANI/CS	1	531	1 M H_2SO_4	[33]
RuO_2	PANI/RuO_2	-	664	1 M H_2SO_4	[33]
RuO_2	RuO_2/SnO_2	-	930	1 M H_2SO_4	[33]
RuO_2	RuO_2/TiO_2	-	534	.5 M H_2SO_4	[33]
RuO_2	RuO_2/Stainless Steel	-	1190	.5 M H_2SO_4	[33]
RuO2·xH2O	$RuO_2 \cdot xH_2O$	1	673.37	1 M H_2SO_4	[33]
RuO2·1.84H2O	$RuO_2 \cdot 1.84H_2O$	.5	511	1 M H_2SO_4	[33]
RuO2·xH2O	$RuO_2 \cdot xH_2O$/Ti	2	840	1 M H_2SO_4	[33]
RuO2·xH2O	$RuO_2 \cdot xH_2O$/C	-	715	1 M H_2SO_4	[33]
RuO2·xH2O	$RuO_2 \cdot xH_2O$/C	-	633	2 M KOH	[33]
RuO2·xH2O	$RuO_2 \cdot xH_2O$/MW CNT	25	1585	1 M H_2SO_4	[33]
RuO2·xH2O	$RuO_2 \cdot xH_2O$/CNT	-	620	1 M H_2SO_4	[33]

1.4.2.2.2 Manganese Oxide

As discussed above ruthenium oxide has proven to be a good material but the cost and toxicity is a great disadvantage. For that reason, many alternatives have been explored. Such as, a combination of composites for ruthenium and alternative metal oxides like manganese oxide. Manganese Oxide is low cost, naturally abundant,environmentally safe and has a high theoretical capacitance[21, 18]. That said, the performance of manganese oxide is dependent on various aspects. Physical properties and chemical factors affect the performance of Mn oxide[29]. Table 1.5 shows different combinations of Mn for pseudocapacitor electrodes. Different types of

synthesis and electrolytes for a variety of combinations of manganese oxides give different specific capacitance.

Table 1.5: Manganese Oxide for pseudocapacitor electrodes

Mn based material	**Electrolyte**	**Method of synthesis**	**Specific capacitance (F g-1)**	**Ref.**
Mn_3O_4/Graphene	-	Hydrothermal	367	[34]
MnO_2 films	-	Sol - gel method	360	[34]
Mn/Ni Oxide	-	Anodic Deposition	250	[34]
Mn/MWCNT	-	Sol- gel method	339	[34]
MnO_2/CNT	.2 M $Na2SO_4$	-	642	[29]
Mn_2O_3/C	6 M KOH	Chemical Process	600	[35]
Mn_2O_3/C	1 M $Na2SO_4$	Hydrothermal	235	[35]
Mn_2O_3/Graphene Oxide	1 M KOH	Reflux method	998.2	[35]
$Mn_2O_3/NiCo_2O_4$ Composite	-	Hydrothermal	824	[35]
Mn_2O_3 Hallow nanotube arrays	1 M KOH	Hydrothermal	677	[35]
Porous Mn_2O_3/C	1 M $Na2SO_4$	Metal-Organic framework	776	[35]

In order to improve the performance of Mn oxides, enhancement in the preparation processes, microstructure, crystallinity, and chemical state of Mn oxides is shown to be an effective approach[29].For the preparation process, Table 1.3 shows various methods that are utilized. Various synthesis are used for electrode material to evaluate which shows a better performance in combination with other factors. It can be seen from Table 1.5 that the hydrothermal process is used the most. The morphology relates to the specific area and the specific capacitance. For that reason, some morphologie in which Mn oxide is prepared are nanowires, nanorods, nanobelts, flower-like microspheres , nanotubes to name a few[29,30]. Ultimately, there is a concentration of research on MnO_2 composites and nanostructured [29].

1.4.2.2.3 Nickel Oxide

Nickel Oxide is another transition metal oxide considered as an alternative to Ruthenium oxide. It has proven to have high theoretical specific capacitance , abundant, low cost, environmental friendly, and easy to synthesize[29]. However, some drawbacks would be low conductivity, and strain is developed in pure NiO during discharge and charge which leads to poor stability. To overcome those drawbacks composites based on NiO are prepared[36]. Table 1.6 shows various synthesis methods and performance of Nickel oxide, Nickel hydroxide.

Table 1.6: Nickel Oxide and Nickel hydroxide electrode-based material

Ni based material	Electrolyte	Method of synthesis	Specific capacitance (F g-1)	Ref.
$Ni(OH)_2$	KOH	-	578	[15]
NiO(Flower like hollow nanospheres)	-	Gas/Liquid interfacial microwave	770	[30]
NiO(Porous Nanocolumns)	-	Hydrothermal	390	[30]
$Ni(OH)_2$/rGO	-	Solvothermal	1886	[34]
NiO/rGO	-	Electrodeposition	950	[34]
NiO	-	Hydrothermal	1700	[34]
$Ni(OH)_2/MnO_2$/rGO	-	Hydrothermal	1985	[34]
Porous nickel oxide/mesoporous carbon	-	Chemical precipitation method	2570	[34]
CNTs/NiO	-	Electrochemical	1701	[36]
Graphene/NiO	-	Chemical vapor deposition followed by adsorption	783	[36]

1.4.2.2.4 Cobalt oxide

Just like the nickel oxide and manganese oxide, Cobalt oxide is abundant, low cost , and environmentally friendly. The four types of cobalt oxides mostly used are CoO,Co_2O_3, CoO_2, and Co_3O_4[37]. From Table 1.7, it can be seen that from the four mentioned before the most common one is Co_3O_4. This is because it has been demonstrated to have good theoretical capacitance. Yet

just like the other metal oxides it has a limitation. The main drawback in cobalt oxide is the low potential window. The low potential window limits its applications [38]. Not only that but, as an electrode material it has poor cycling stability and rate performance. Even though cobalt oxide has many advantages, more research has to be done to make its electrochemical performance better.

Table 1.7: Cobalt Oxide based electrode-based material

Co based material	**Method of synthesis**	**Specific capacitance (F g-1)**	**Ref.**
Co_3O_4	Sol-gel	291	[30]
Co_3O_4(Nanorods)	Microwave assisted hydrothermal	456	[30]
Co_3O_4(Nanotube)	Chemically depositing	574	[30]
Co_3O_4 (brush like nanowires)	Self-organization	1525	[30]
Co_3O_4–MnO_2–NiO nanotubes	Electrodeposition	2525	[34]
$CoMoO_4$ nanoplate arrays	Hydrothermal	1558	[34]

1.4.2.3 Conducting Polymers

Conducting polymers have been studied for the past twenty years due to the low cost, faradic redox capabilities, and a higher energy density than metal oxides[19]. The most common for supercapacitors are polyaniline (PANI), polypyrrole(PPy), Polyacetyylene(PA), and PEDOT.

Having said that, conducting polymers have three configurations for its use in supercapacitors. Type one is symmetric and uses the same p-dopable polymer for both electrodes. Type two is asymmetric, it uses two different p-dopable polymers with different ranges of electroactivity. The third is symmetric, where both electrodes are p-doped for a positive electrode. As for the negative electrode, both are n-doped[39].

An interesting characteristic in conducting polymers that attracts researchers is the doping-dedoping behavior. For this reason, they have been used in various devices such as batteries, supercapacitors and sensors. Figure 1.9 shows a schematic of n-type and p-type doping. It can be seen that the dopant ions convey charge in the form of excess electrons and neutralize the unstable polymer backbone in the oxidized form either by donating or accepting electrons [30]. The doping is used to increase the conductivity, but it also causes its cycling to decrease. This is because the doping and dedoping causes the electrode to deteriorate. Other methods are also used for example, to increase electrical conductivity and capacitance, composites of conduction polymers with other materials are used. These materials include carbon nanotubes, graphene, and metal oxides.

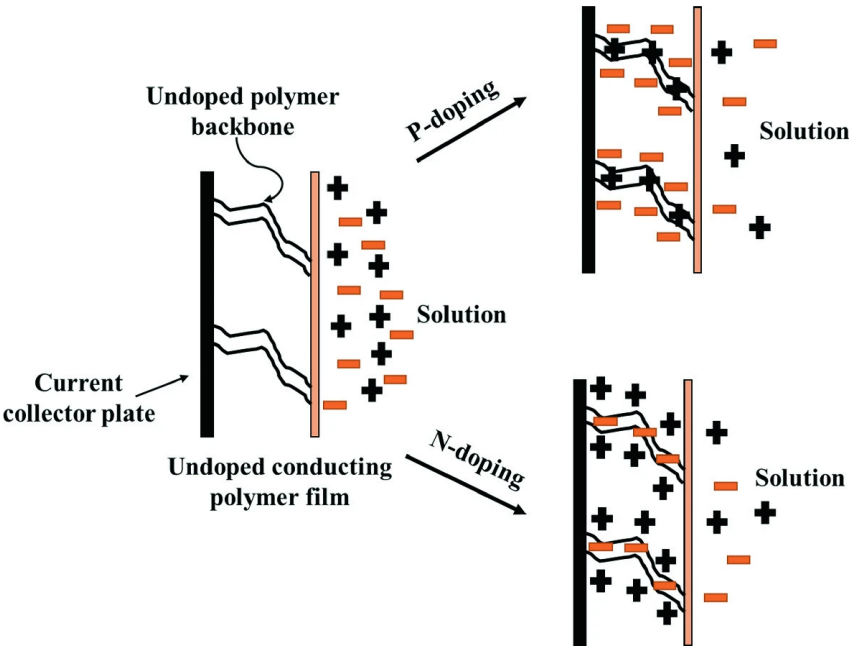

Figure 1.9 : *P*-type and *N*-type doping in conducting polymers[30]

1.4.2.4 Composites

Composite supercapacitor combines the materials of both electric double layer and pseudocapacitor. They are two types of composites, binary and ternary. Binary composites use two different electrode materials to form one electrode [40]. For example, a combination of a carbon material with a metal oxide or conducting polymer. Ternary composites use three different electrode materials to form one electrode[40]. Specifically, a metal oxide, conducting polymer and a carbon material. The use of binary and ternary composites allow the electrode performance to be enhanced. Carbon, metal oxides and conducting polymers have advantages and disadvantages. The combination of materials can help improve the drawbacks a single electrode material might have.

1.4.3 Electrolyte

Generally electrolytes are sorted into two groups, as either liquid or solid. As shown in Figure 1.10, Liquid electrolytes branch out to aqueous and non aqueous. As for solid, it branches into dry polymer, gel polymer and inorganic. With an extensive range of electrolytes, choosing one is essential for the performance of the supercapacitor. The function of the electrolyte is to provide ionic conductivity and allow charge compensation on each electrode. Also, it contributes in the formation of the electrical double layer as well as the reversible redox reaction in pseudocapacitors [41]. With this in mind, to choose an electrolyte it must have a wide voltage window, electrochemical stability, high ionic concentration, low solvated ionic radius, low viscosity, low volatility, low toxicity, low cost, and availability at high purity[21]. Lastly, since the electrolyte interacts with electrodes it is necessary to be mindful of the pairing between electrolyte and electrode material.

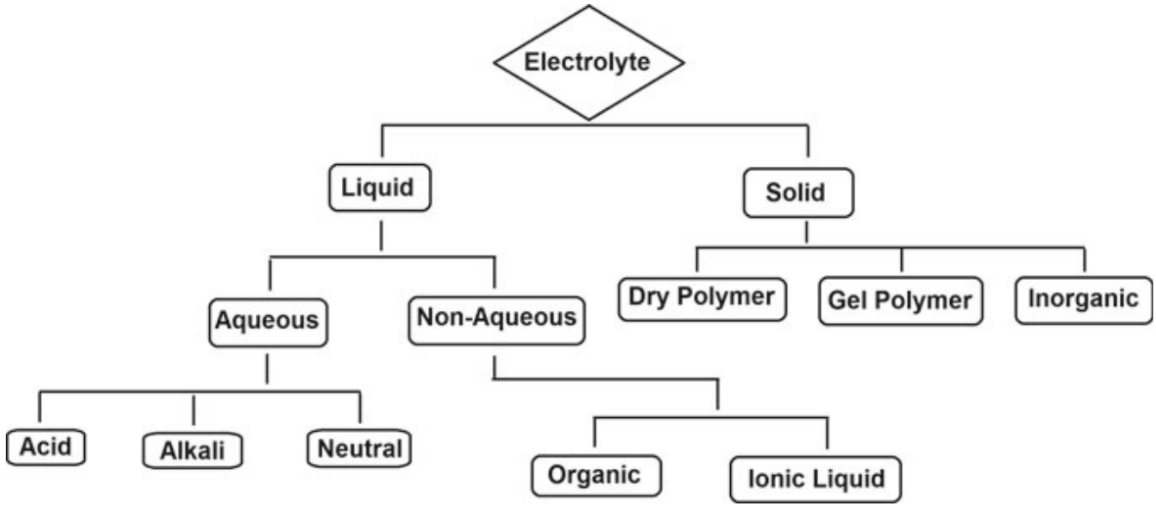

Figure 1.10: Types of electrolytes [18]

1.4.3.1 Aqueous

The most commonly used aqueous electrolytes are H_2SO_4, KOH, Na_2SO_4, and KCl . These electrolytes are low cost, high ionic conductivity, non corrosive, non flammable, and abundant[15, 42]. Another convenient aspect of aqueous electrolytes is that it does not require any special conditions like organic and ionic liquid electrolytes[41]. This makes it easier to make as well as more cheap. Yet, despite these advantages it is usually not used for commercial applications. This is because the voltage window is low compared to other electrolytes. Usually, the voltage window is around 1.2 V. If the voltage was to be increased the cell would deteriorate because of the building of pressure and water decomposition[15].

Aqueous electrolyte can be divided into subsections, acid, alkali and neutral. These three subsections have different pH levels. The most common acid electrolyte used is H_2SO_4, due to its high ionic conductive nature. The conductivity mainly relies on concentration.For example, for carbon based supercapacitors the highest conductivity attains from 1 M of H_2SO_4 at 25 degrees celsius. [43]. That said, many metal oxides are not good for acid electrolyte for that reason alkaline electrolytes are used. [43]. The most common alkaline electrolytes are KOH, LiOH and NaOH. Out of these three the most researched is KOH due to the high conductivity. [18]. Lastly, neutral electrolytes have a greater operating window and are safer than acidic and alkaline electrolytes. The most commonly used neutral electrolyte for research is Na_2SO_4. [43]

1.4.3.2 Organic

Organic electrolytes require strict process conditions to obtain ultra pure products[42]. This is because the procedure requires a meticulous environment to prevent any impurities that can cause self- discharge as well as degradation issues. Regardless of these conditions it is used

for commercially available supercapacitors. This is because of its high potential window in the range of 2.5-2.8 V [19]. Usually, organic electrolytes for commercial use consist of TEABF4 dissolved in solvents such as ACN and PC [41]. In other words, a conducting salt dissolved in a solvent. Even though organic electrolytes have a high potential window, they also possess low conductivity, and small specific capacitance. As well as high cost, volatile, toxic and flammable[19].

1.4.3.3 Ionic Liquid

Ionic liquid electrolytes are molten salts composed of ions of melting points below 100 degrees celsius[41]. The low melting attributes to the asymmetric organic cation and inorganic/organic anion[38]. Some of the advantages are high thermal, chemical and electrochemical stability, negligible volatility, and non flammability[41]. Furthermore, ionic liquid electrolytes are classified as aprotic protic and zwitterionic[38]. The figure 1.11 shows the most commonly used cations and anions of ionic liquid electrolyte. The combinations of the anions and cations are vast.

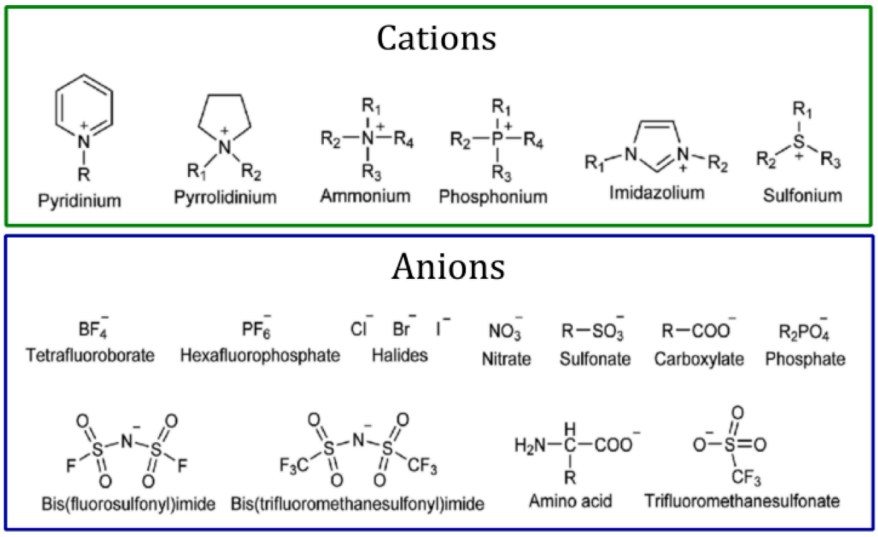

Figure 1.11: Commonly used cations and anions of ionic liquids [43]

1.4.3.4 Solid State Polymer

A solid polymer is solvent free and it is composed of a polymer and a salt[38]. Besides, leakage is a major concern in certain applications, a solid state electrolyte can help with that. Moreover, with an increase in portable devices such as wearable electronics, printable electronics, flexible electronics, and micr-electronics, the need of a solid state electrolyte is of great need[9]. Supercapacitors derived from solid polymer electrolytes have high electrochemical stability, good working temperature, high mechanical strength, and structural stability[18]. A polymer based solid electrolyte is divided into three subsections, solid polymer, gel polymer and polyelectrolyte. Out of the three, gel polymer electrolyte has the highest ionic conductivity. For that reason they are the most used in solid based electrolytes[9].

1.4.4 Supercapacitor System

In previous sections, the types of supercapacitors were mentioned. The types of supercapacitors are EDLC, pseudocapacitor and hybrid. The types of supercapacitors pertain to the materials of the electrodes. In this section, the supercapacitor device will be discussed. Depending on the structure of the supercapacitor device, it can be classified into symmetric, asymmetric, and hybrid. In a symmetric system, the supercapacitor is made up of two electrodes with identical materials. For example, activated carbon for the positive and negative electrodes. Another example is ruthenium oxide on both electrodes. In an asymmetrical system, the electrodes are made up of two different capacitive materials. For example, one electrode can be of carbon material and the other electrode can be of a different carbon material. Another example would be as shown in Table 1.8, one electrode is made of a metal oxide and the other electrode is made of a carbon material. As for a hybrid system, the supercapacitor has one electrode made of

either a EDLC or pseudocapacitor and the other electrode is battery type. As shown below, nickel and cobalt oxides and hydroxides are shown as a battery like material and are not evaluated as a pseudocapacitive material [44].

Table 1.8: Supercapacitor systems examples

Symmetric		
Positive electrode	**Negative electrode**	**Ref.**
AC	AC	[48
RuO_2	RuO2	[48]
Asymmetric		
Positive electrode	**Negative electrode**	**Ref.**
MnO_2	AC	[47]
MnO_2	CNT's	[47]
MnO_2	Activated graphene	[47]
MnO_2/ CNT's	CNT's	[47]
MnO_2/CNT	AC	[47]
Mn_3O_4/graphene	CNTs/graphene	[47]
RuO_2/graphene	Graphene	[47]
PANi/CNTs/graphene	Graphene	[47]
Hybrid		
Positive electrode	**Negative electrode**	[47]
CuO	AC	[47]
NiO	Reduced graphene oxide	[47]
$Ni(OH)_2$	AC	[47]
$Co(OH)_2$	AC	[47]
Co_3O_4	AC	[47]
$Co3O_4$	Graphene	[47]
$NiCo_2O_4$	AC	[44]
$NiMoO_4$	AC	[44]

1.4.5 Characterization Methods

1.4.5.1 Physical

1.4.5.1.1 Brunauer-Emmett Teller (BET)

The brunauer-emmett teller (BET) method is often used to determine the surface area, and pore size distribution. The BET method is based on the physical adsorption of gas molecules on the surface of the sample being tested. This at a range of pressures that covers the monolayer coverage of molecules[46]. This method usually uses inert gasses such as Nitrogen or Argon as adsorbates to quantify the surface area[47].These gasses are used in most cases because they are nonreactive gas molecules. Meaning the gasses will not chemically react with the material being studied. Carbon dioxide can also be used but usually for specific surface areas with pore diameters of less than 1nm[45].

1.4.5.1.2 X-ray Photoelectron Spectroscopy (XPS)

X-ray Photoelectron Spectroscopy (XPS) is a physical characterization method used to evaluate the surface chemistries of electrode materials[48]. It is a very important technique because pseudocapacitor type electrodes rely on faradic surface reactions. In addition, reactions happening at the surfaces of materials such as oxides, semiconductors, glasses, ceramics, polymers, composites and biomaterials can be evaluated[49]. Some elements that are used in an XPS instrument are a X-ray source, an electron energy analyzer and ultra high vacuum environment[50]. As shown in Figure 1.12, the x-rays will come in contact with the sample. Then the X-ray photons will knock out the valence electrons but only if the photon has a higher

energy to overcome the binding energy of the electrode. This will cause the electron to move with some kinetic energy[51].

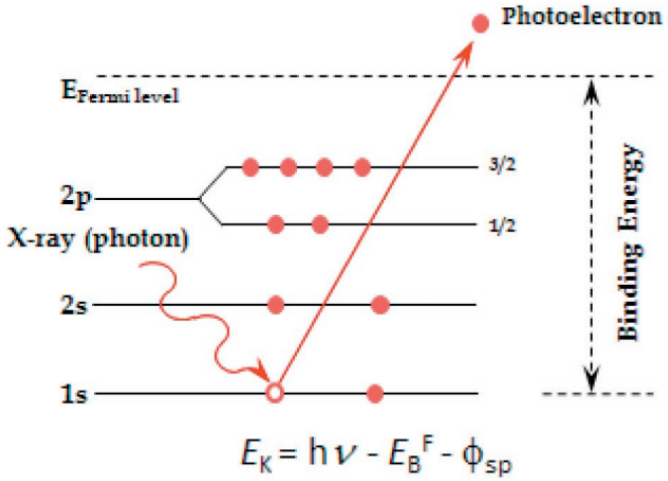

Figure 1.12: Schematic of photoelectric effect [50]

To calculate the kinetic energy the potential and the kinetic energy will be equal to each other meaning, conservation of energy. The detector will provide a stopping potential and the kinetic energy can be calculated. From the kinetic energy the binding energy can then be determined. Leading to the development of a plot like shown in Figure 1.13, showing the number of photoelectrons detected or intensity and binding energy. Each peak from the XPS plot can identify the elements because each element has a characteristic set of binding energy [50].

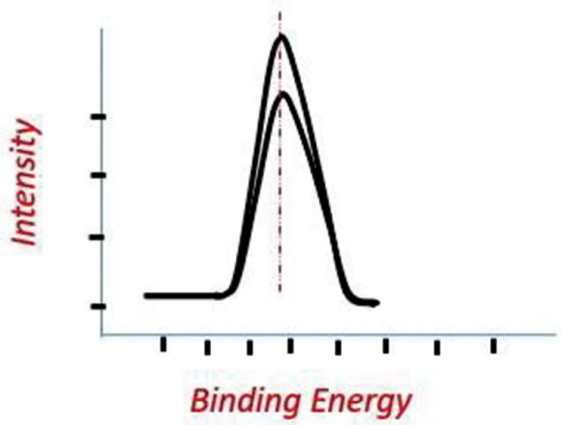

Figure 1.13: Schematic of an XPS peak [51]

1.4.5.1.3 X-ray diffraction (XRD)

X-ray diffraction (XRD) is a technique used to examine elemental analysis, phase analysis, stress measurements and texture analysis[52].This method works when radiation hits a solid or crystalline material and a diffraction pattern forms that displays its characteristics [53]. Having said that, Figure 1.14 shows an example of a XRD output. To analyze the output of an XRD test, the peak position, intensity, and shape have to be considered. Through the peak position, lattice parameters, space group, chemical composition, macrostresses, or qualitative phase analysis can be assessed. From the peak intensity, the crystal structure, texture and quantitative phase analysis can be attained. As for the peak shape or width, it can indicate the microstrains and the crystalline size [54].

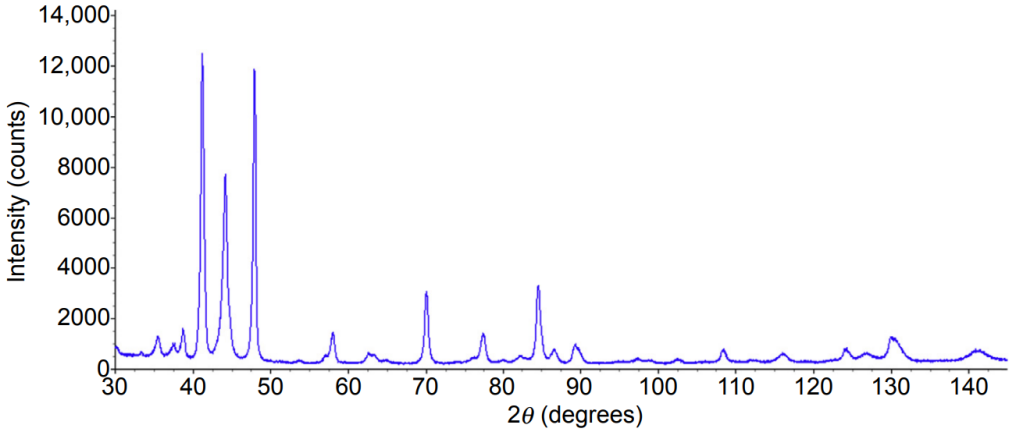

Figure 1.14: XRD plot example [54]

1.4.5.1.4 Scanning electron microscopy (SEM)

Scanning electron microscopy (SEM) is a technique used to produce magnified images to study the microstructure and surface morphology of a material[Characterization of biomaterial]. Its magnification can reach 300,000x and in newer models it can reach 1,000,000 [51]. Having said that, an electron beam is scanned across the sample and a variety of interactions occur between the beam and the material.[55]. Figure 1.15, shows the modes that can be used for images and characterization of the sample. For example, the composition of the material can be attained by examining the x-rays generated from the interaction between the electron and the sample. Also, the morphology images are attained by collecting secondary electrons with nanoscale resolution [55].

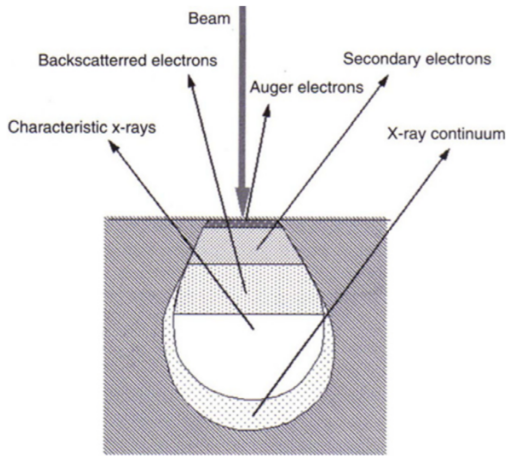

Figure 1.15: Schematic of electron-material interaction [55]

1.4.5.1.5 Fourier Transform Infrared (FTIR)

In FTIR a IR light is directed into a sample that repeats the exposure over various frequency ranges. Some wavelengths will be reflected but most of it will pass through the sample. From the light that was not reflected some of it will be absorbed by the material and the other part will be transmitted. The IR light that is transmitted or absorbed is then measured by a detector. This detector will measure the light that was either absorbed or transmitted. The results are given in an absorption or transmitted, and wavelength graph. To analyze the information the shape, position and peak intensity are observed. The analysis will derive from commercial libraries [52].

1.4.5.2 Electrochemical

To test the electrochemical cell in a lab a two or three electrode configuration is implemented. A three electrode system is composed of a working electrode (WE), a reference electrode (RE), and a counter electrode(CE). The working electrode is the electrode with the material being tested. The reference electrode is used as a constant potential. The counter

electrode is used to complete the electric circuit. In a two electrode configuration only the counter electrode and working electrode are used. Figure 1.16 shows a basic schematic of a two and three electrode configuration.

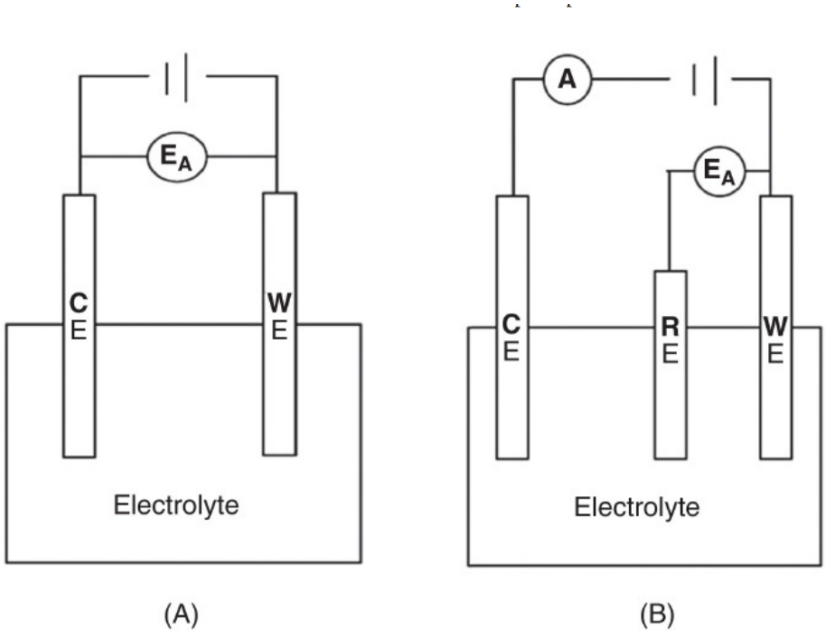

Figure 1.16: schematic of (A) two electrode (B) three electrode configurations [56]

In essence, the current flows through the counter electrode to the working electrode. The voltage is measured between the reference and the working electrodes. Since the two electrode configuration does not have a reference electrode the voltage measure will be the cell voltage [57]. Having said that, the changes observed in the two-electrode configuration is for the entire cell. As for the three electrode configuration, it is used to observe changes in the working electrode against the reference electrode [58]. Certain reference electrodes used are Hg/Hg_2Cl_2, $Hg/HgSO_4$, Ag/AgCl, Hg/HgO, and $Ag/AgNO_3$. For the counter electrode platinum wire or graphite rods are commonly used[48].

1.4.5.2.1 Cyclic Voltammetry (CV)

This technique is used for qualitative and pseudo-qualitative studies, kinetic analysis by scanning a wide range of scan rates, and voltage window determination [57]. Since actual devices require greater capacity this technique is used in laboratories with smaller samples. Cyclic voltammetry is occasionally utilized to analyze a single electrode using either a two or three electrode system. The working principle is applying a potential range at some scan rate and observing the current between that potential range. Basically, a positive voltage charges to the maximum voltage established. For example, if the potential difference set is from 0-1 then the maximum voltage would be 1. After the maximum voltage is achieved the process is reversed for discharging. Usually, the measurements are formed using a linear sweep pattern or a cyclic profile [58]. Hence, a plot of current as a function of potential difference for a specific scan rate is generated.

An ideal cyclic voltammetry representation of EDLC, pseudocapacitors and faradaic of the different types of supercapacitor materials is shown in Figure 1.17 . The electric double layer can be recognized from the rectangular shape shown in the figure above[59]. It can be seen from the voltammogram of the pseudocapacitors that it is not rectangular but, rather, looks a little distorted. The faradaic reactions are causing the shape to be quasi-rectangular. Also, the relationship between time and the applied potential is shown.

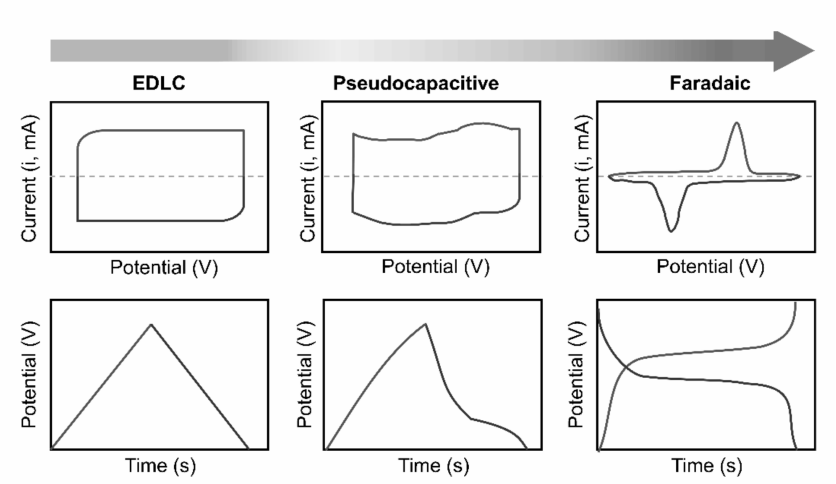

Figure 1.17: CV and GCD schematic [59]

The CV can be used to calculate the average capacitance for an EDLC. It can also be used for a pseudocapacitor that displays a behavior similar to a rectangular curve. However, the average capacitance cannot be calculated from the CV if it displays faradic behaviors. Having said that, equation 1 shows the equation that can be used to find the capacitance for an EDLC.

$$C = \frac{\int i\, dV}{2v\Delta V} \qquad \textbf{(1)}$$

Where, the numerator accounts for the total area under the CV curve, v is the scan rate, and ΔV is the potential difference. It is divided by 2 because it accounts for discharge only. Now from that, the specific capacitance of the electrode can be found using equation 2.

$$Cs = \frac{C}{m} \qquad \textbf{(2)}$$

Where, C is the capacitance of the electrode cell, and m is the mass of the active material. It should be noted that the specific capacitance can be divided by mass, volume, or area.
Cyclic voltammetry is helpful for evaluating cyclability and the operating potential window of an electrode. When the potential ranges are increased the stability can be monitored as well as the safe operating potential window. The safe operating window can be determined from the anodic

and cathodic peaks. Degradation of the electrode and electrolyte decomposition can be seen when peaks in the voltammetry are not normal. As stated in the electrolyte section, the different electrolytes have different operating ranges. If the voltages are outside the window this will cause electrolyte decomposition. Something which will cause a device to be damaged [56].

Furthermore, the scan rate controls how quickly the potential is scanned [60]. Slower or lower scan rates allow better contact of electrolyte and electrode material but it usually takes a longer time for testing. Also, lower or slower scan rates and lower current densities show higher capacitance. Fast scan rates often show lower capacitance. Ultimately, cyclic voltammetry is useful to determine the potential window for supercapacitor materials. This, by adjusting the parameters used and studying the charge and discharge processes [56]. Yet it is usually used in combination with the GCD technique [48]. The GCD technique will be discussed in the next section.

1.4.5.2.2 Galvanostatic charge/ discharge (GCD)

Galvanostatic charge/ discharge (GCD) is a test that records the change in voltage as a function of time while keeping a fixed current[58]. The voltage window that is used is determined in the cyclic voltammetry test. This is why CV and GCD are commonly used together. Figure 1.17 shows the schematic of CV and GCD. The top being the CV and the bottom the GCD. Furthermore, the specific capacitance of an electrode can be calculated using equation 3.

$$C = \frac{I \cdot \Delta t}{\Delta V \cdot A} \qquad \textbf{(3)}$$

Where, C is the capacitance, I is the fixed current, Δt is the discharge time, ΔV is the voltage window and A is the area. Area can be substituted to volume or mass. Next, the internal resistance drop can be calculated using equation 4.

$$R = \frac{Vdrop}{\Delta I} \quad \textbf{(4)}$$

Where, V_{drop} is the voltage drop and ΔI is the section in which the current is interrupted.When the current is interrupted it is linked to the resistance of the cell[56]. In part due to various aspects such as ionic resistance from the electrolyte, electrode resistance, faradaic reactions on the electrode surface, active material and current collector interaction[58]. Figure 1.18 shows the illustration of the internal resistance drop.

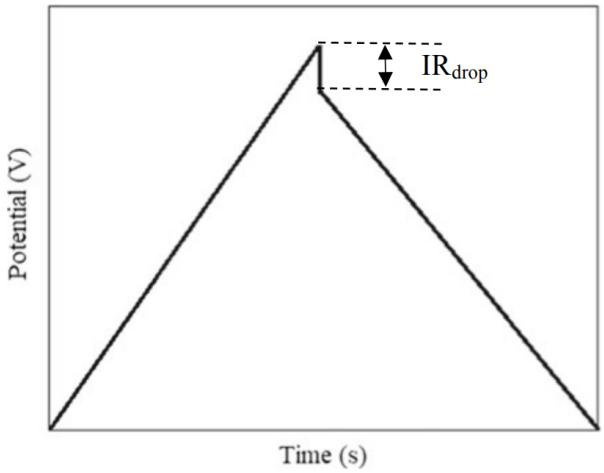

Figure 1.18: Internal resistance drop illustration [58]

Essentially, this method is used to evaluate the performance of supercapacitors such as capacitance, energy density, power density, ESR and cycle stability [19]. As shown above the capacitance is analyzed using eq. 3. In addition, the capacitance for different currents can be calculated. With that information a graph for specific capacitance as a function of current can be created. It should be noted that specific currents should reflect real life applications [26]. The energy density and power density will be discussed in later sections. As for ESR, the internal

resistance can be evaluated using eq.4. Lastly, the cycle stability can be attained by comparing the capacitance of thousands of cycles with that of the first cycle [56].

1.4.5.2.3 Electrochemical impedance spectroscopy(EIS)

The next characterization method is electrochemical impedance spectroscopy. In the impedance spectroscopy, a potential or current is applied to a fixed frequency. The response is measured and the impedance is computed for several frequencies. This method has been used because it gives detailed information about impedance, internal resistance, current responses, and capacitance [26]. Generally, the information is represented in a Bode plot and a Nyquist plot. The bode plot is used to evaluate capacitive systems while the Nyquist plot is used to evaluate resistive processes [61]. Figure 1.19 shows a circuit model of a porous carbon electrode. From graph (A), in the Nyquist plot, term one and two are dependent on the electrolyte. Number three is controlled by both the electrode material and the electrolyte [56].

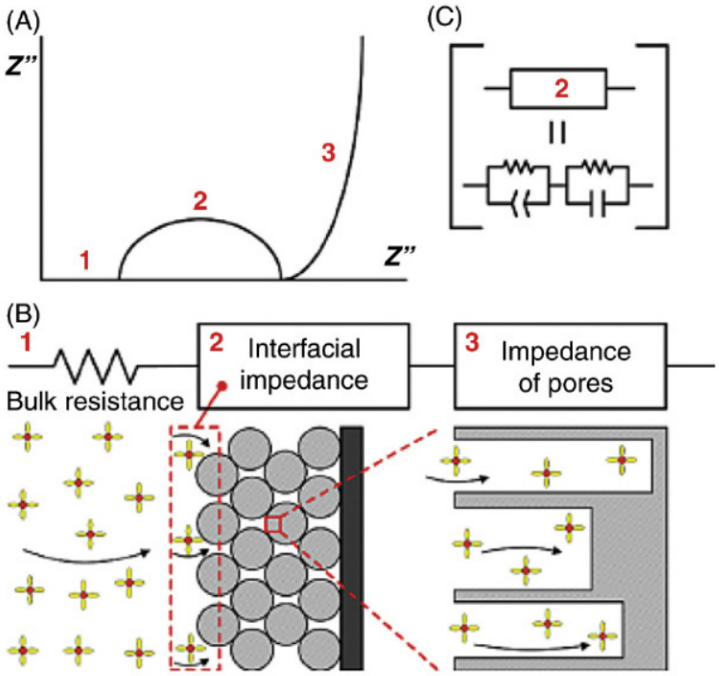

Figure 1.19 : Porous carbon electrode EIS schematic [56]

As stated above and as shown in Figure 1.20, Nyquist plot is composed of three regions. The first one is represented as a semicircle at high frequencies, usually larger than 10^4. This semicircle commonly shows interface resistance. The next region is the high to medium frequency, usually between 10^4-1 Hz. This region shows charge transfer resistance. The last region is at low frequencies, usually less than 1Hz. This region usually indicates the capacitive behavior [48]. R. Ahmed et al. reported based on this knowledge, that the MoNi-5 nanowires sample shows a smaller resistance during charge transfer [62]. As shown in Figure 1.20, (b) section is a zoomed in plot of plot (a). It can be seen that the diameter of MoNi-5 is smaller than the other samples. Normally, a bigger diameter will show a larger value of resistance. For this reason, it can be implied that MoNi-5 shows a smaller resistance in comparison to the other samples.

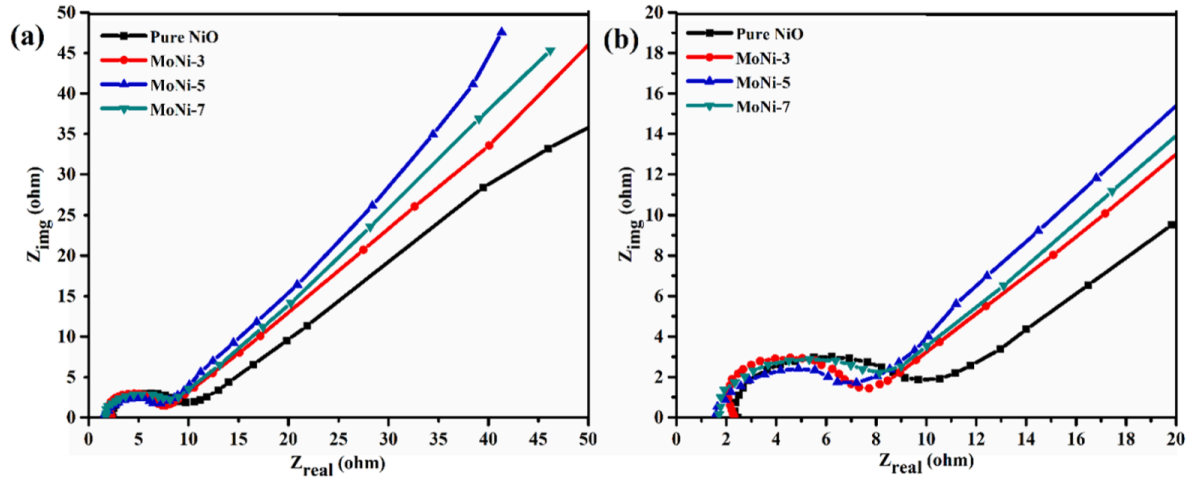

Figure 1.20: Nyquist plot of Mo-Doped NiO nanowires [62]

1.4.5.3 Energy Density

Energy density is the amount of energy stored per unit mass or volume of the device. Batteries exhibit a high energy density and supercapacitors exhibit lower energy densities in

comparison to batteries. This is a major drawback for supercapacitors. Equation 5 shows the formula for energy density.

$$E = \frac{Cs \cdot (\Delta V)^2}{2} \quad \textbf{(5)}$$

Where, C_s is the specific capacitance , ΔV is the voltage applied or potential window.
From eq. 5 it can be concluded that, to increase energy density, either capacitance or potential window need to be increased. The capacitance can be increased from the electrode material. For instance, the surface area, pore size, electrical conductivity. The potential window can be widened by using an electrolyte such as organic or ionic liquid. Organic electrolyte can achieve cell voltage of 2.5-2.8 V and ionic liquid can be as high as 3.5 V. Also asymmetric and hybrid supercapacitors can be used. If the energy density of supercapacitors is improved then it can be an alternative for batteries.

1.4.5.4 Power Density

Power density describes the speed at which energy is stored or given off[26.] Unlike energy density, batteries exhibit a lower power density and supercapacitors exhibit a higher power density. Yet, even though supercapacitors exhibit a superior power density, batteries are the choice for commercial energy storage devices. This is because they have a higher energy density. In order to have supercapacitors further commercialized then its power density has to be kept high but also the energy density has to be improved. The equation for power density is shown below.

$$P = \frac{E}{\Delta t} \quad \textbf{(6)}$$

Where, E is the energy density, Δt is the discharge time. It is an advantage that supercapacitors have and for that reason it is seen as an alternative for batteries.

1.4.6 Research gap and novelty of work

There were different approaches researchers have used to overcome the poor electrical conductivity. Nickel oxides- carbon composites and bi-metal oxides composites and doping in nickel oxides etc. have been tried. Among all the surface fictionalization of transition metal oxides is a simple and efficient approach. surface fictionalization in nickel oxides enhances the electrical conductivity, creates an efficient diffusion path, and introduces oxygen vacancies, all of which improve overall supercapacitor performance. To the best of our knowledge, it's the first time trying to incorporate germanium in a nickel oxides matrix to improve the electrochemical performance in supercapacitors application.

CHAPTER 2 : EXPERIMENTAL SECTION

2.1 Chemicals and Reagents

All chemical reagents were of reagent grade and have been used without any further purification. Potassium hydroxide (KOH), Hydrochloric acid (37%), Nickel sulfate hexahydrate ($NiSO_4.6H_2O$), Ammonium Chloride (NH_4Cl), Polyethylene glycol, and Copper (99.98%), were purchased from Sigma-Aldrich. Distilled water has been used in all experiments for making solutions and cleaning.

2.2 Electrodeposition of Microporous Ni

The growth of microporous nickel on copper substrate was carried out using the Galvanostatic electrodeposition process. The electrodeposition was performed using two electrode setup, where nickel foam and copper substrate were used as a counter and working electrode, respectively. Prior to the deposition, copper substrate was cleaned in 1M HCl solution and deionized water. The bath for the synthesis of microporous nickel was prepared by adding 0.12M Nickel sulfate hexahydrate, 1 M Ammonium Chloride and polyethylene glycol (100 mg in 300 ml) in deionised water. Then, the beaker containing aqueous bath was sonicated for 5 min to get a stable light green solution. The electrodeposition was done at current 100 $mAcm^{-2}$ for 3 min. After the deposition, samples were cleaned in deionized water and kept at 60°C for 1 h in an oven.

2.3 RF-Sputtering of Germanium on Microporous Ni

RF-sputtering was used to deposit germanium on the 3-D porous nickel network for 2, 4, 6 and 8 minutes. After that all samples were annealed at 400°C for 30 min.

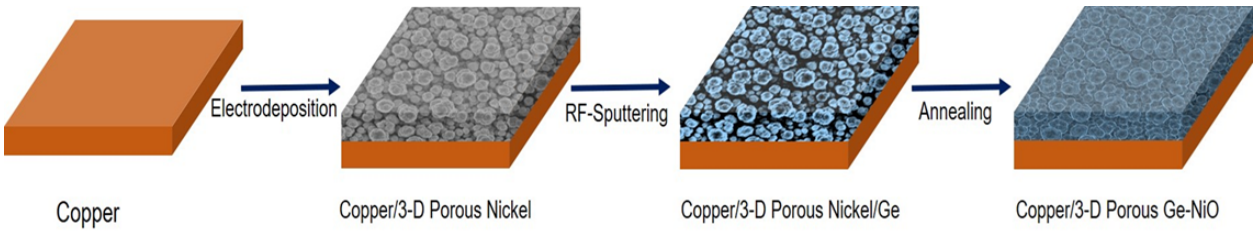

Figure 2.1: Schematic for 3-D mesoporous Ge-NiO

CHAPTER 3: RESULTS AND DISCUSSION

3.1 Structure, Morphology and Elemental Composition

3.1.1 Crystal Structure and Phase

It can be seen in figure 3.1 the result for the x-ray diffraction. The peaks correspond to copper and nickel. Also, it can be noted that NiO is not present. There is a possibility that the peaks for the NiO are situated in the same position as Ni.

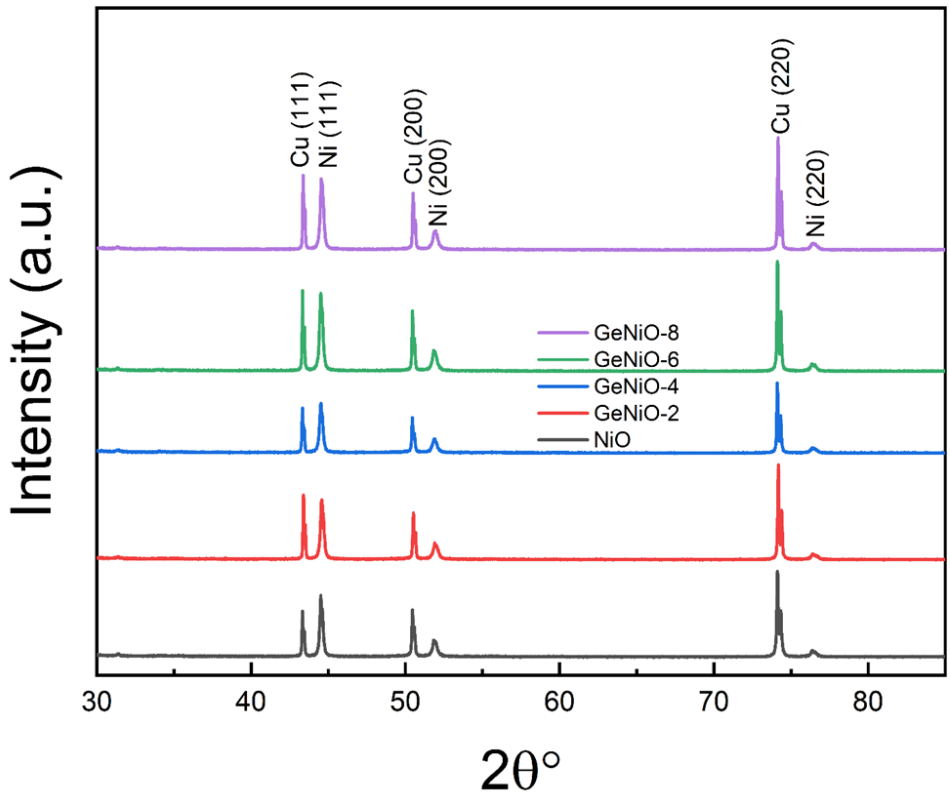

Figure 3.1: X-ray diffraction pattern of 3-D mesoporous Nickel-Germanium-Nickel Oxides on copper substrate after annealing 400°C for 30 min.

3.1.2 Surface Morphology

The scanning electron microscopy gives a better understanding of the surface morphology. It can be seen from figure 3.2 that it is a cauliflower structure. Also, it shows that (a) and (b)

corresponding to nano porous nickel and NiO are sharper in the edges. Once germanium is deposited it becomes less sharp with the increase of the deposition of the germanium.

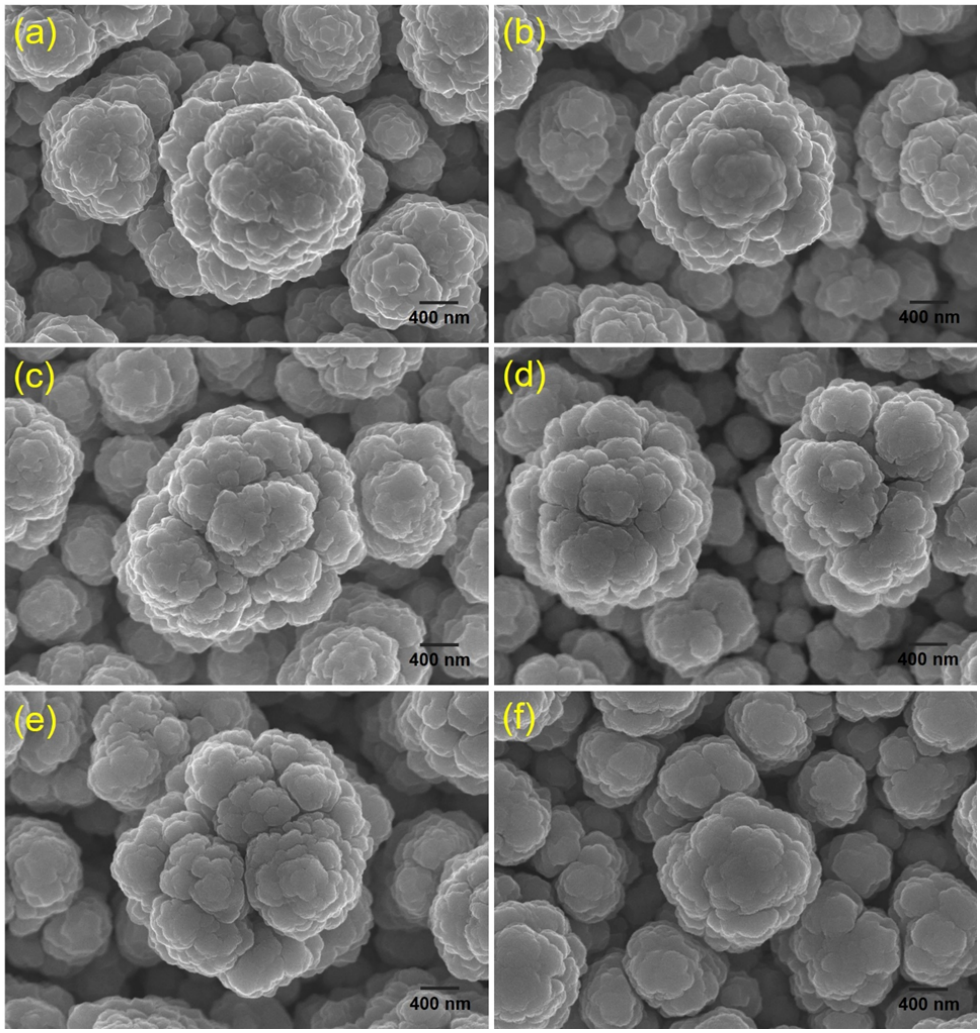

Figure 3.2: SEM images of (a)electrodeposited nickel oxide nanoflakes on 3-D microporous nickel and after annealing 400°C for 30 min (b) NiO (c) GeNiO-2, (d) GeNiO-4, (e) GeNiO-6 and (f) GeNiO-8.

3.1.3 Elemental Composition and Homogeneity

The EDS analysis shows the distribution of the elements present in the material, as shown in figure 3.3. The images are obtained using the SEM and used in this EDS analysis. With that being said, the red color indicates the elemental mapping of nickel. The green color shows the oxygen and lastly, the blue color shows germanium. Based on the Elemental composition analysis it can be seen that with the increase of the deposition time germanium is more concentrated in the top surface of the cauliflower structure.

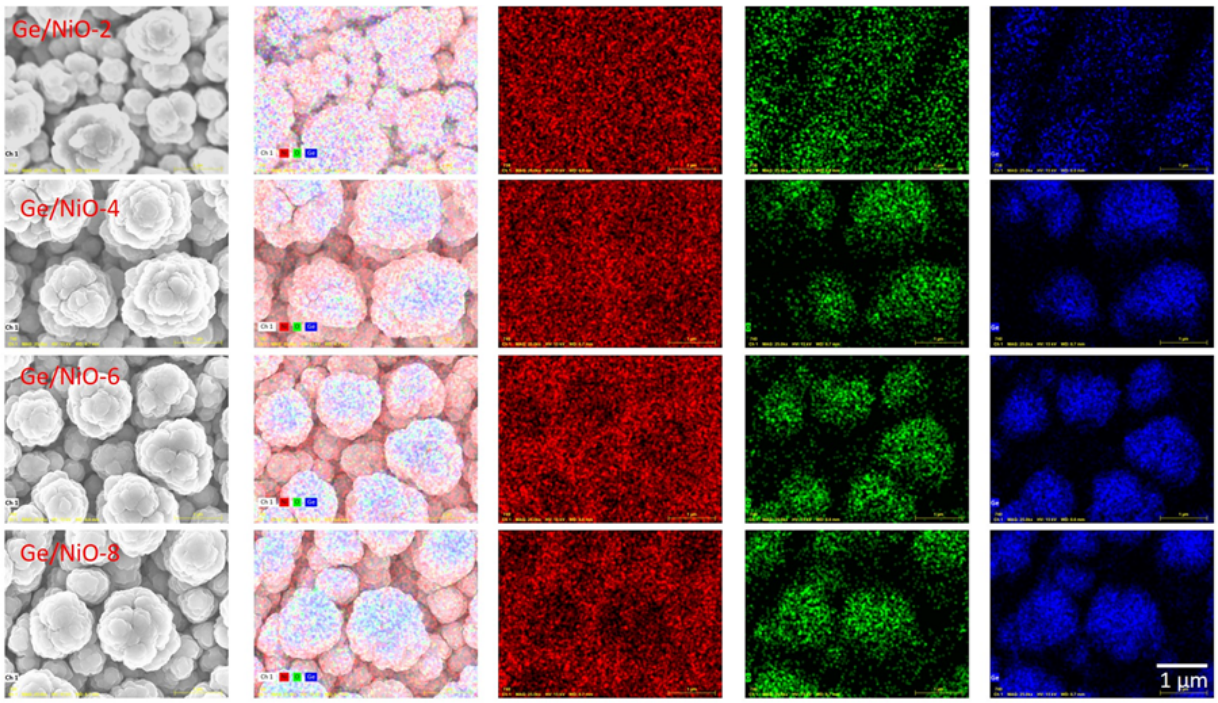

Figure 3.3: EDX elemental mapping of 3-D mesoporous Nickel-Germanium-Nickel Oxides with different deposition time of Germanium and after annealing 400°C for 30 min (a)-(d) GeNiO-2, (f)-(j) GeNiO-4, (k)-(o) GeNiO-6 and (p)-(t) GeNiO-6.

3.2 Electrochemical Characterization

3.2.1 Cyclic Voltammetry

The cyclic voltammetry of Ge-NiO at different deposition times and scan rates is shown in figure 3.4. The deposition times are 2,4,6, and 8 minutes and the scan rates range from 2-200mVs^{-1}. In addition, it can be seen that the results display anodic and cathodic peaks which indicate pseudocapacitive behavior. The CV was done in a three electrode system, where platinum was used as the counter electrode, and Hg/HgO was used as the reference electrode. From the potential vs current density the specific capacitance can be calculated for different scan rates. This can be done by dividing the area under the curve by the scan rate and voltage window. Also it can be normalized by mass, volume, or area. From the specific capacitance calculated graph (f) is obtained. It can be seen that the sample Ge-NiO-4 shows a higher specific capacitance when compared to the other deposition times.

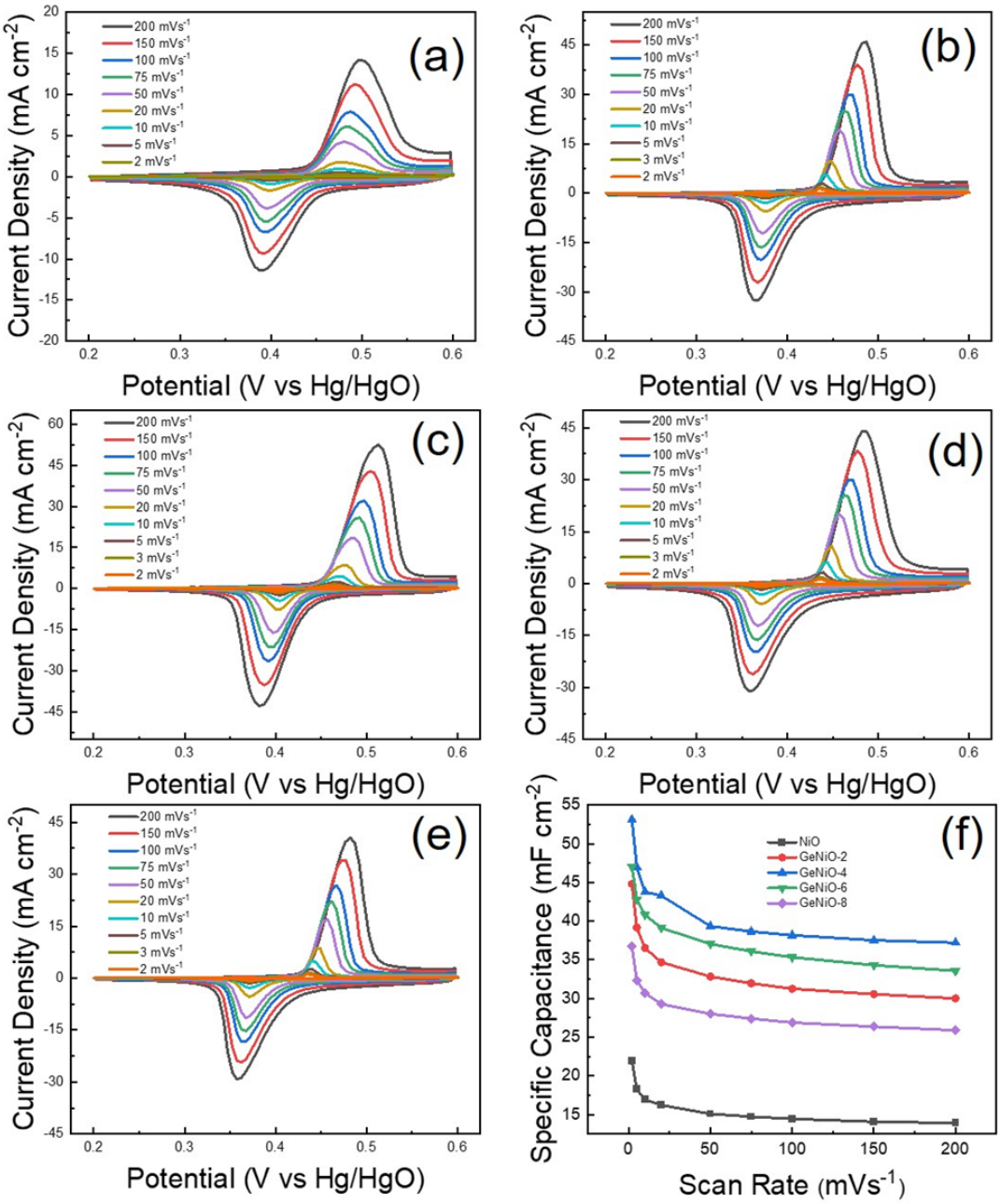

Figure 3.4: Cyclic Voltammetry of 3-D mesoporous Nickel-Germanium-Nickel Oxides with different deposition time of Germanium and after annealing 400°C for 30 min (a) NiO, (b) GeNiO-2, (c) GeNiO-4, (d) GeNiO-6, (e) GeNiO-6 and (f) comparisons of specific capacitance at different scan rates.

3.2.2 Galvanic Charge-Discharge Profiles

The galvanic charge and discharge profiles are shown in figure 3.5. It can be seen that the time is higher at Ge-NiO with a deposition of 4 min. This means more energy. Since capacitance is proportional to discharge time at constant current density, the capacitance is higher with higher time. For this reason Ge-NiO- 4 displays a higher specific capacitance.

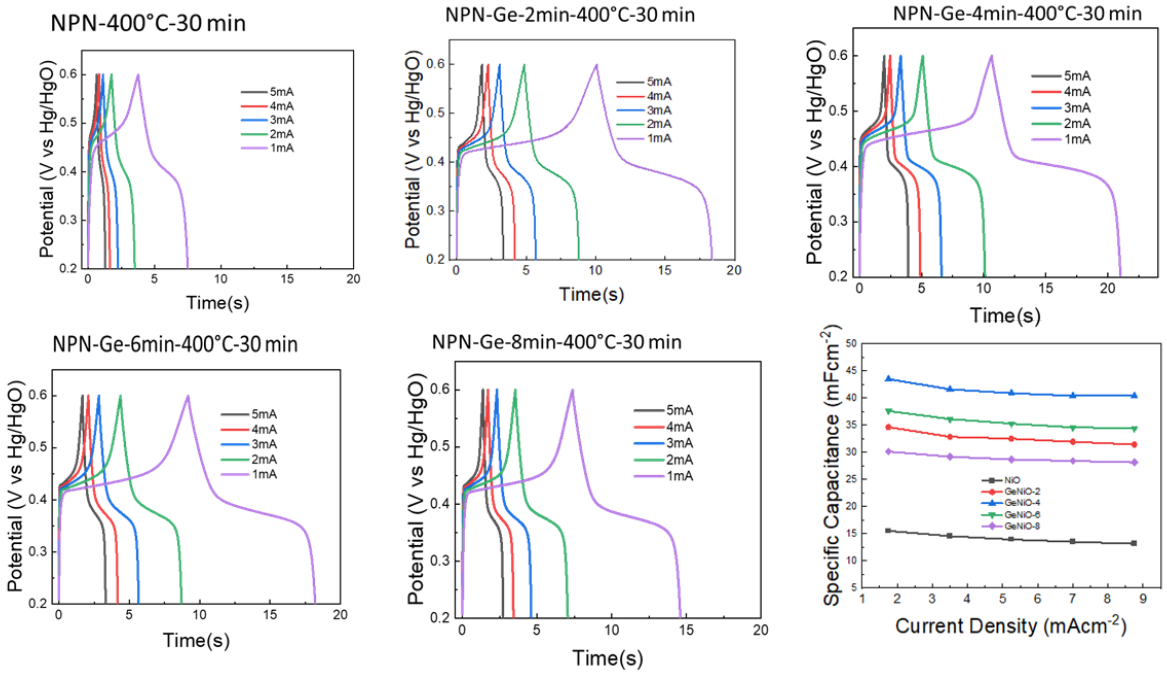

Figure 3.5: Galvanic Charge-discharge of 3-D mesoporous Nickel-Germanium-Nickel Oxides with different deposition time of Germanium and after annealing 400°C for 30 min (a) NiO, (b) GeNiO-2, (c) GeNiO-4, (d) GeNiO-6, (e) GeNiO-6 and (f) comparisons of specific capacitance at different current density.

3.2.3 Cyclic Stability

The cyclic stability is done to check the stability of the material. In NPN the cyclic stability is degrading meaning that the NiO alone without Germanium has a poor cyclic stability. Once the germanium is deposited it can be seen that it becomes more stable.

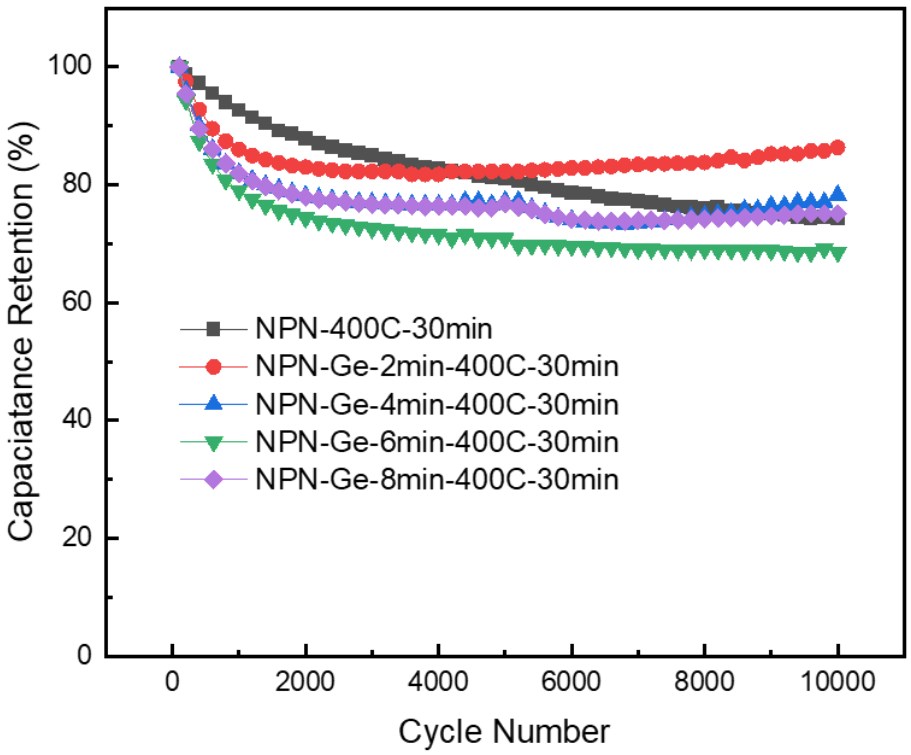

Figure 3.6: Cyclic stability of 3-D mesoporous Nickel-Germanium-Nickel Oxides with different deposition time of Germanium and after annealing 400°C for 30 min.

3.3 Cyclic Voltammetry of Activated Carbon

The negative electrode for the asymmetric supercapacitor will be activated carbon. Activated carbon was tested with different drying times to compare their specific capacitance. It can be seen from figure 3.7 that the activated carbon dried at 60 ℃ showed better results. For that reason, the activated carbon dried at 60 ℃ will be used for the negative electrode in the asymmetric supercapacitor.

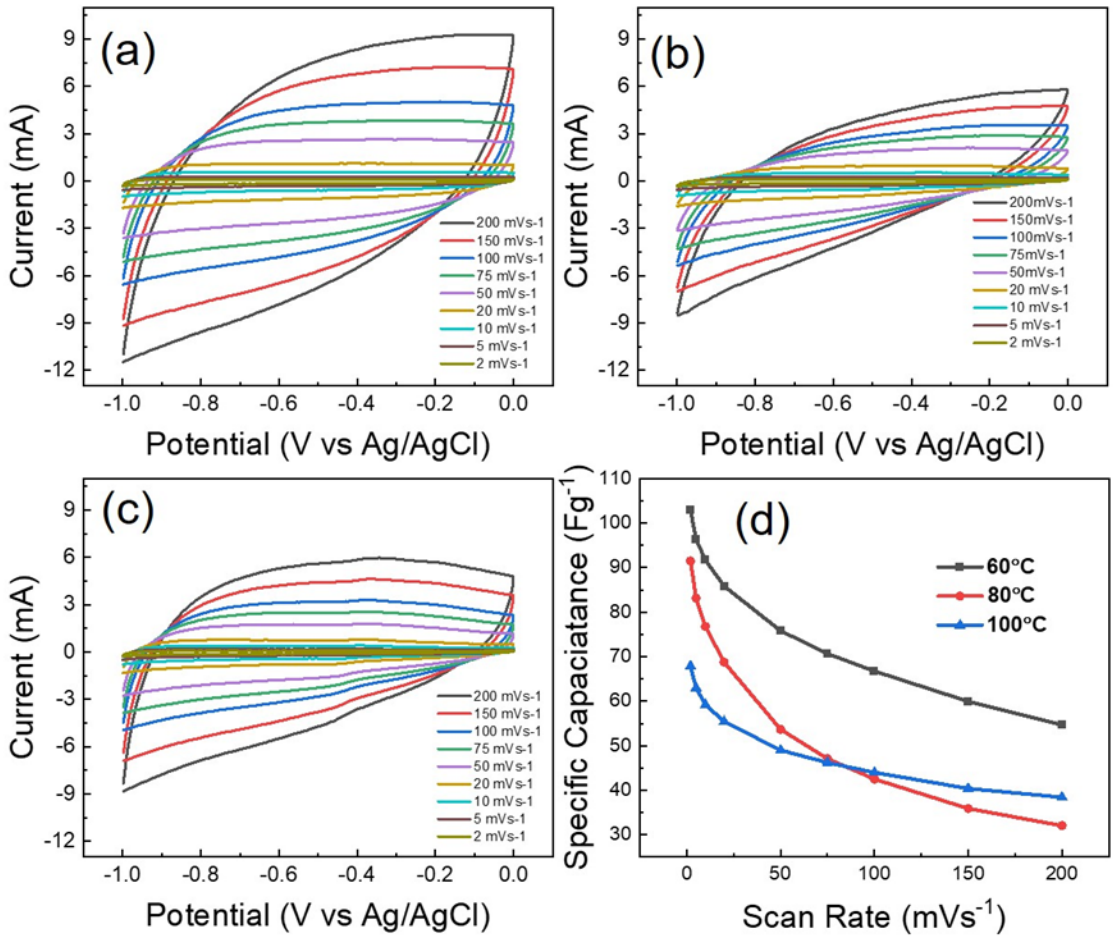

Figure 3.7: Cyclic Voltammetry of activated carbon tested in 1M KOH after drying at different conditions (a) 60°C (b) 80°C, (c) 100°C and (d) comparisons of specific capacitance at different scan rates.

3.4 Asymmetric Supercapacitor

The asymmetric supercapacitor was fabricated using Ge-NiO-4 because it showed better performance when compared with other deposition times. As for the negative electrode, activated carbon dried at 60 ℃ is used due to better results. That said, figure 3.8 shows the electrochemical characterization of the asymmetric supercapacitor composed of Ge-NiO and activated carbon. In figure 3.7 it can be seen that activated carbon is stable at -1-0 V and figure 3.4 shows that Ge-NiO-4 is stable at .2-.6 V. The potentials are added which gives around 1.6V, as shown in figure 3.8 (c). The cyclic voltammetry and galvanic charge/discharge results are shown in figure 3.8 (c) and (d). From the CV and GCD the capacitance, energy density and power density can be calculated. Then, a Ragone plot or power density vs energy density plot can be made. After making the asymmetric supercapacitor the energy and power density improved as shown in figure 3.8 (f).

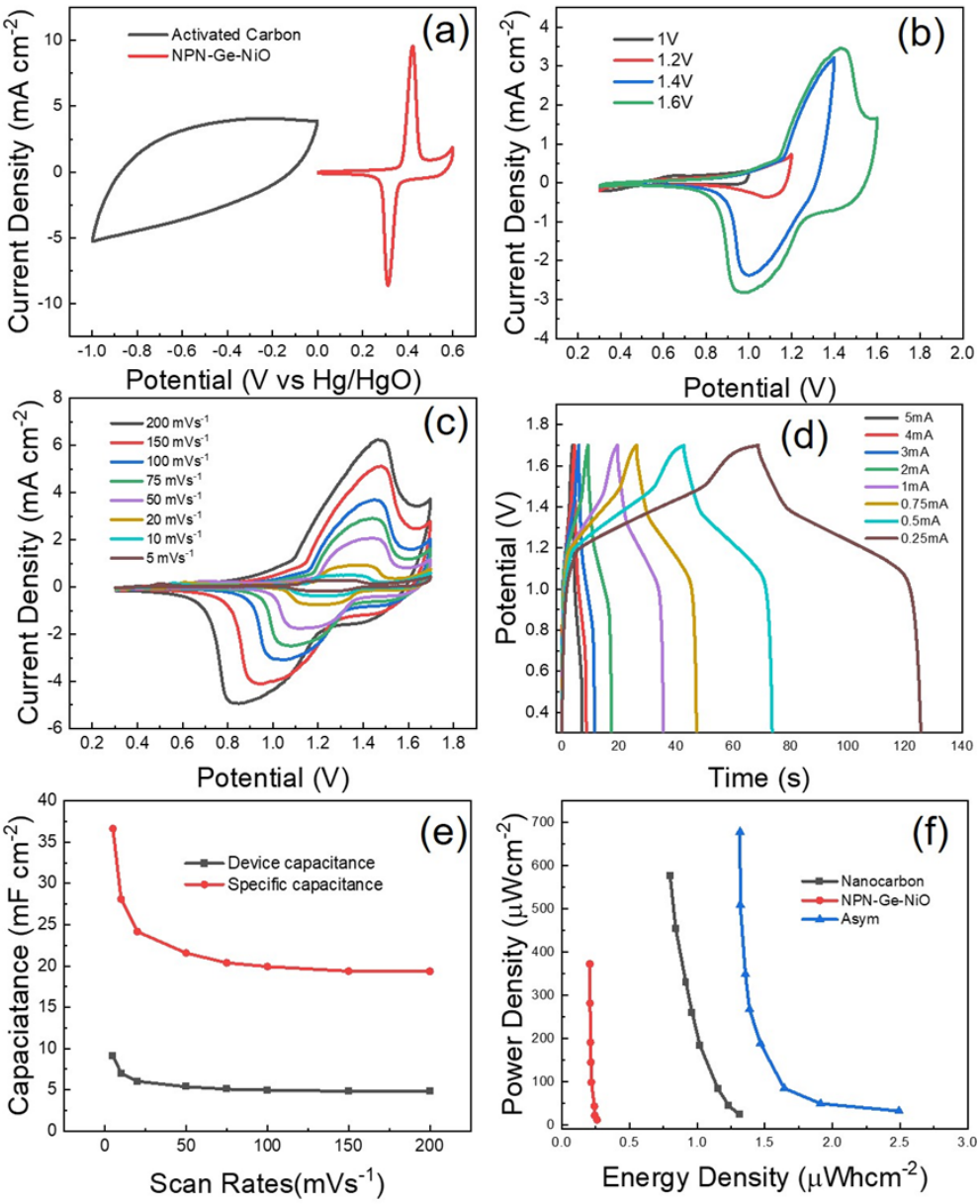

Figure 3.8: Electrochemical characterization of Nickel-Germanium-Nickel Oxides// Activated Carbon asymmetric supercapacitor

In order to test the asymmetric supercapacitor a charge and discharge test was done. From figure 3.9 the image from the left shows the supercapacitor charging. The image on the right shows the supercapacitor discharging. First the asymmetric supercapacitor was charged at 5mA and then it was discharged through a watch. It can be seen that it was able to power the watch for 4 minutes.

Figure 3.9: Practical demonstration of Nickel-Germanium-Nickel Oxides// Activated Carbon asymmetric supercapacitor (a) charging and (b) discharging at 1 mA current.

CHAPTER 4: FUTURE WORK

In this thesis an alkaline electrolyte was used. For future work it would be beneficial to test germanium functionalized nickel oxide in different electrolytes. For example, acidic or organic. Then compare their performance for supercapacitors. Also, test germanium functionalized nickel oxides for electrocatalysis and battery applications. Lastly, it would be interesting to fabricate, optimize and study other metal oxides. For instance, cobalt oxide, and manganese oxide. Then compare their performance with NiO.

CHAPTER 5 : CONCLUSION

In the present work, we successfully demonstrate the improvement in performance of supercapacitors by incorporation of germanium at the 3-D mesoporous nickel/ nickel oxides interface. The electrodeposition, RF-sputtering and annealing were done to fabricate germanium functionalize nickel oxides on 3-D mesoporous nickel framework. The 3-D mesoporous nickel with interconnected framework provides high surface area and excellent ionic conductivity. Germanium improves the electrical conductivity of nickel oxides by reducing charge transfer resistance. Germanium incorporation in 3-D nickel and nickel oxides interface enhanced the specific capacitance of nickel oxides by more than twice. The asymmetric supercapacitor shows the specific capacitance of 36 $mFcm^{-2}$, energy density of 2.5 $\mu Whcm^{-2}$, and power density of 0.67 $mWcm^{-2}$. The asymmetric supercapacitor has enabled digital watches to run for several minutes, demonstrating practical application of the device.

LIST OF REFERENCES

[1] U.S. Energy Information Administration. U.S. Energy Facts Explained - Consumption and Production - U.S. Energy Information Administration (EIA) https://www.eia.gov/energyexplained/us-energy-facts/.

[2] Wuebbles, D. J.; Easterling, D. R.; Hayhoe, K.; Knutson, T.; Kopp, R. E.; Kossin, J. P.; Kunkel, K. E.; LeGrande, A. N.; Mears, C.; Sweet, W. V.; Taylor, P. C.; Vose, R. S.; Wehner, M. F. Ch. 1: Our Globally Changing Climate. Climate Science Special Report: Fourth National Climate Assessment, Volume I. 2017. https://doi.org/10.7930/j08s4n35.

[3] Fu, L.; Ren, Z.; Si, W.; Ma, Q.; Huang, W.; Liao, K.; Huang, Z.; Wang, Y.; Li, J.; Xu, P. Research Progress on CO2 Capture and Utilization Technology. *Journal of CO2 Utilization* 2022, *66*, 102260. https://doi.org/10.1016/j.jcou.2022.102260.

[4] Fang, H.; Li, D.; Zhao, M.; Zhang, Y.; Yang, J.; Wang, K. Research Progress and Prospect of Hybrid Supercapacitors as Boosting the Performance. Energy Sources, Part A: Recovery, Utilization, and Environmental Effects 2022, 1–18. https://doi.org/10.1080/15567036.2022.2033887

[5] Olabi, A. G.; Abbas, Q.; Al Makky, A.; Abdelkareem, M. A. Supercapacitors as next Generation Energy Storage Devices: Properties and Applications. *Energy* 2022, *248*, 123617. https://doi.org/10.1016/j.energy.2022.123617.

[6] Gautham Prasad, G.; Shetty, N.; Thakur, S.; Rakshitha; Bommegowda, K. B. Supercapacitor Technology and Its Applications: A Review. *IOP Conference Series: Materials Science and Engineering* 2019, *561*, 012105. https://doi.org/10.1088/1757-899x/561/1/012105.

[7] Libich, J.; Máca, J.; Vondrák, J.; Čech, O.; Sedlaříková, M. Supercapacitors: Properties and Applications. *Journal of Energy Storage* 2018, *17*, 224–227. https://doi.org/10.1016/j.est.2018.03.012.

[8] Faraji, S.; Ani, F. N. The Development Supercapacitor from Activated Carbon by Electroless Plating—a Review. *Renewable and Sustainable Energy Reviews* 2015, *42*, 823–834. https://doi.org/10.1016/j.rser.2014.10.068.

[9] Scibioh, M. A.; Viswanathan, B. Electrolyte Materials for Supercapacitors. *Materials for Supercapacitor Applications* 2020, 205–314. https://doi.org/10.1016/b978-0-12-819858-2.00004-4.

[10] Miller, E. E.; Hua, Y.; Tezel, F. H. Materials for Energy Storage: Review of Electrode Materials and Methods of Increasing Capacitance for Supercapacitors. *Journal of Energy Storage* 2018, *20*, 30–40. https://doi.org/10.1016/j.est.2018.08.009.

[11] Burt, R.; Birkett, G.; Zhao, X. S. A Review of Molecular Modelling of Electric Double Layer Capacitors. *Physical Chemistry Chemical Physics* 2014, *16* (14), 6519. https://doi.org/10.1039/c3cp55186e.

[12] Wang, H.; Pilon, L. Accurate Simulations of Electric Double Layer Capacitance of Ultramicroelectrodes. *The Journal of Physical Chemistry C* 2011, *115* (33), 16711–16719. https://doi.org/10.1021/jp204498e.

[13] Waqas Hakim, M.; Fatima, S.; Rizwan, S.; Mahmood, A. Pseudo-Capacitors: Introduction, Controlling Factors and Future. *Nanostructured Materials for Supercapacitors* 2022, 53–70. https://doi.org/10.1007/978-3-030-99302-3_3.

[14] Yu, A.; Chabot, V.; Zhang, J. *Electrochemical Supercapacitors for Energy Storage and Delivery*; CRC Press, 2017.

[15] Muzaffar, A.; Ahamed, M. B.; Deshmukh, K.; Thirumalai, J. A Review on Recent Advances in Hybrid Supercapacitors: Design, Fabrication and Applications. *Renewable and Sustainable Energy Reviews* 2019, *101*, 123–145. https://doi.org/10.1016/j.rser.2018.10.026.

[16] Liew, S. Q.; Jun, H. K. Fundamentals, Mechanism, and Materials for Hybrid Supercapacitors. *Nanostructured Materials for Supercapacitors* 2022, 71–100. https://doi.org/10.1007/978-3-030-99302-3_4.

[17] Afif, A.; Rahman, S. M.; Tasfiah Azad, A.; Zaini, J.; Islan, M. A.; Azad, A. K. Advanced Materials and Technologies for Hybrid Supercapacitors for Energy Storage – a Review. *Journal of Energy Storage* 2019, *25*, 100852. https://doi.org/10.1016/j.est.2019.100852.

[18] *Handbook of Nanocomposite Supercapacitor Materials I*; Kar, K. K., Ed.; Springer International Publishing: Cham, 2020. https://doi.org/10.1007/978-3-030-43009-2.

[19] Raza, W.; Ali, F.; Raza, N.; Luo, Y.; Kim, K.-H.; Yang, J.; Kumar, S.; Mehmood, A.; Kwon, E. E. Recent Advancements in Supercapacitor Technology. *Nano Energy* 2018, *52*, 441–473. https://doi.org/10.1016/j.nanoen.2018.08.013.

[20] Chang, S.-K.; Zainal, Z. Activated Carbon for Supercapacitors. *Synthesis, Technology and Applications of Carbon Nanomaterials* 2019, 309–334. https://doi.org/10.1016/b978-0-12-815757-2.00012-7.

[21] González, A.; Goikolea, E.; Barrena, J. A.; Mysyk, R. Review on Supercapacitors: Technologies and Materials. *Renewable and Sustainable Energy Reviews* 2016, *58*, 1189–1206. https://doi.org/10.1016/j.rser.2015.12.249.

[22] Manasa, P.; Sambasivam, S.; Ran, F. Recent Progress on Biomass Waste Derived Activated Carbon Electrode Materials for Supercapacitors Applications—a Review. *Journal of Energy Storage* 2022, *54*, 105290. https://doi.org/10.1016/j.est.2022.105290.

[23] Yin, L.; Chen, Y.; Li, D.; Zhao, X.; Hou, B.; Cao, B. 3-Dimensional Hierarchical Porous Activated Carbon Derived from Coconut Fibers with High-Rate Performance for Symmetric Supercapacitors. *Materials & Design* 2016, *111*, 44–50. https://doi.org/10.1016/j.matdes.2016.08.070.

[24] Jalal, N. I.; Ibrahim, R. I.; Oudah, M. K. A Review on Supercapacitors: Types and Components. *Journal of Physics: Conference Series* 2021, *1973* (1), 012015. https://doi.org/10.1088/1742-6596/1973/1/012015.

[25] REVATHI, S.; Vuyyuru, M.; Dhanaraju, M. D. CARBON NANOTUBE: A FLEXIBLE APPROACH FOR NANOMEDICINE AND DRUG DELIVERY. *Asian J Pharm Clin Res* 2015, *8*, 25-31.

[26] *Nanostructured Materials for Supercapacitors*; Thomas, S., Gueye, A. B., Gupta, R. K., Eds.; Springer International Publishing: Cham, 2022. https://doi.org/10.1007/978-3-030-99302-3.

[27] Graphene Synthesis, Characterization and Its Applications: A Review. *Results in Chemistry* 2021, *3*, 100163. https://doi.org/10.1016/j.rechem.2021.100163

[28] Geim, A. K.; Novoselov, K. S. The Rise of Graphene. *Nature Materials* 2007, *6* (3), 183–191. https://doi.org/10.1038/nmat1849.

[29] Scibioh, M. A.; Viswanathan, B. Electrode Materials for Supercapacitors. *Materials for Supercapacitor Applications* 2020, 35–204. https://doi.org/10.1016/b978-0-12-819858-2.00003-2.

[30] Kar, K. K. *Handbook of Nanocomposite Supercapacitor Materials II*; Springer Nature, 2020.

[31] Zhou, L.; Li, C.; Liu, X.; Zhu, Y.; Wu, Y.; van Ree, T. Metal Oxides in Supercapacitors. *Metal Oxides in Energy Technologies* 2018, 169–203. https://doi.org/10.1016/b978-0-12-811167-3.00007-9.

[32] Lenar, N.; Paczosa-Bator, B.; Piech, R. Optimization of Ruthenium Dioxide Solid Contact in Ion-Selective Electrodes. *Membranes* 2020, *10* (8), 182. https://doi.org/10.3390/membranes10080182.

[33] Li, Q.; Zheng, S.; Xu, Y.; Xue, H.; Pang, H. Ruthenium Based Materials as Electrode Materials for Supercapacitors. *Chemical Engineering Journal* 2018, *333*, 505–518. https://doi.org/10.1016/j.cej.2017.09.170.

[34] Mu. Naushad; Rajendran, S.; Al-Enizi, A. M. *New Technologies for Electrochemical Applications*; CRC Press, 2020.

[35] Parveen, N.; Ansari, S. A.; Ansari, M. Z.; Ansari, M. O. Manganese Oxide as an Effective Electrode Material for Energy Storage: A Review. *Environmental Chemistry Letters* 2021. https://doi.org/10.1007/s10311-021-01316-6.

[36] Sk, M. M.; Yue, C. Y.; Ghosh, K.; Jena, R. K. Review on Advances in Porous Nanostructured Nickel Oxides and Their Composite Electrodes for High-Performance Supercapacitors. *Journal of Power Sources* 2016, *308*, 121–140. https://doi.org/10.1016/j.jpowsour.2016.01.056.

[37] Mei, J.; Liao, T.; Ayoko, G. A.; Bell, J.; Sun, Z. Cobalt Oxide-Based Nanoarchitectures for Electrochemical Energy Applications. *Progress in Materials Science* 2019, *103*, 596–677. https://doi.org/10.1016/j.pmatsci.2019.03.001.

[38] Kate, R. S.; Khalate, S. A.; Deokate, R. J. Overview of Nanostructured Metal Oxides and Pure Nickel Oxide (NiO) Electrodes for Supercapacitors: A Review. *Journal of Alloys and Compounds* 2018, *734*, 89–111. https://doi.org/10.1016/j.jallcom.2017.10.262.

[39] Snook, G. A.; Kao, P.; Best, A. S. Conducting-Polymer-Based Supercapacitor Devices and Electrodes. *Journal of Power Sources* 2011, *196* (1), 1–12. https://doi.org/10.1016/j.jpowsour.2010.06.084.

[40] M. Aulice Scibioh; Viswanathan, B. *Materials for Supercapacitor Applications*; Elsevier, 2020.\

[41] Zhong, C.; Deng, Y.; Hu, W.; Sun, D.; Han, X.; Qiao, J.; Zhang, J. *Electrolytes for Electrochemical Supercapacitors*; CRC Press, 2016.

[42] Sarno, M. Nanotechnology in Energy Storage: The Supercapacitors. *Studies in Surface Science and Catalysis* 2020, 431–458. https://doi.org/10.1016/b978-0-444-64337-7.00022-7.

[43] Iqbal, M. Z.; Zakar, S.; Haider, S. S. Role of Aqueous Electrolytes on the Performance of Electrochemical Energy Storage Device. *Journal of Electroanalytical Chemistry* 2020, *858*, 113793. https://doi.org/10.1016/j.jelechem.2019.113793.

[44] Shao, Y.; El-Kady, M. F.; Sun, J.; Li, Y.; Zhang, Q.; Zhu, M.; Wang, H.; Dunn, B.; Kaner, R. B. Design and Mechanisms of Asymmetric Supercapacitors. *Chemical Reviews* 2018, *118* (18), 9233–9280. https://doi.org/10.1021/acs.chemrev.8b00252.

[45] Wang, Y.; Song, Y.; Xia, Y. Electrochemical Capacitors: Mechanism, Materials, Systems, Characterization and Applications. *Chemical Society Reviews* 2016, *45* (21), 5925–5950. https://doi.org/10.1039/c5cs00580a.

[46] Sinha, P.; Datar, A.; Jeong, C.; Deng, X.; Chung, Y. G.; Lin, L.-C. Surface Area Determination of Porous Materials Using the Brunauer–Emmett–Teller (BET) Method: Limitations and Improvements. *The Journal of Physical Chemistry C* 2019, *123* (33), 20195–20209. https://doi.org/10.1021/acs.jpcc.9b02116.

[47] Nasrollahzadeh, M.; Atarod, M.; Sajjadi, M.; Sajadi, S. M.; Issaabadi, Z. Plant-Mediated Green Synthesis of Nanostructures: Mechanisms, Characterization, and Applications. *Interface Science and Technology* 2019, 199–322. https://doi.org/10.1016/b978-0-12-813586-0.00006-7.

[48] Baig, M. M.; Gul, I. H.; Baig, S. M.; Shahzad, F. The Complementary Advanced Characterization and Electrochemical Techniques for Electrode Materials for Supercapacitors. *Journal of Energy Storage* 2021, *44*, 103370. https://doi.org/10.1016/j.est.2021.103370.

[49] Wagner, J. M. *X-Ray Photoelectron Spectroscopy*; Nova Science Publishers: New York, 2011.

[50] Engelhard, M. H.; Droubay, T. C.; Du, Y. X-Ray Photoelectron Spectroscopy Applications. *Encyclopedia of Spectroscopy and Spectrometry* 2017, 716–724. https://doi.org/10.1016/b978-0-12-409547-2.12102-x.

[51] Kumar, R. *Surface Characterization Techniques*; Walter de Gruyter GmbH & Co KG, 2022.

[52] Nasrazadani, S.; Hassani, S. Modern Analytical Techniques in Failure Analysis of Aerospace, Chemical, and Oil and Gas Industries. *Handbook of Materials Failure Analysis with Case Studies from the Oil and Gas Industry* 2016, 39–54. https://doi.org/10.1016/B978-0-08-100117-2.00010-8.

[53] Khan, H.; Yerramilli, A. S.; D'Oliveira, A.; Alford, T. L.; Boffito, D. C.; Patience, G. S. Experimental Methods in Chemical Engineering: X‐Ray Diffraction Spectroscopy— XRD. *The Canadian Journal of Chemical Engineering* 2020, *98* (6), 1255–1266. https://doi.org/10.1002/cjce.23747.

[54] Epp, J. X-Ray Diffraction (XRD) Techniques for Materials Characterization. *Materials Characterization Using Nondestructive Evaluation (NDE) Methods* 2016, 81–124. https://doi.org/10.1016/b978-0-08-100040-3.00004-3.

[55] Sampath Kumar, T. S. Physical and Chemical Characterization of Biomaterials. *Characterization of Biomaterials* 2013, 11–47. https://doi.org/10.1016/b978-0-12-415800-9.00002-4.

[56] Scibioh, M. A.; Viswanathan, B. Characterization Methods for Supercapacitors. *Materials for Supercapacitor Applications* 2020, 315–372. https://doi.org/10.1016/b978-0-12-819858-2.00005-6.

[57] Lu, M. *Supercapacitors : Materials, Systems, and Applications*; Wiley: Weinheim, 2013.

[58] Eleri, O. E.; Lou, F.; Yu, Z. Characterization Methods for Supercapacitors. *Nanostructured Materials for Supercapacitors* 2022, 101–128. https://doi.org/10.1007/978-3-030-99302-3_5.

[59] Aderyani, S.; Flouda, P.; Shah, S. A.; Green, M. J.; Lutkenhaus, J. L.; Ardebili, H. Simulation of Cyclic Voltammetry in Structural Supercapacitors with Pseudocapacitance Behavior. *Electrochimica Acta* 2021, *390*, 138822. https://doi.org/10.1016/j.electacta.2021.138822.

[60] Elgrishi, N.; Rountree, K. J.; McCarthy, B. D.; Rountree, E. S.; Eisenhart, T. T.; Dempsey, J. L. A Practical Beginner's Guide to Cyclic Voltammetry. *Journal of Chemical Education* 2017, *95* (2), 197–206. https://doi.org/10.1021/acs.jchemed.7b00361.

[61] Magar, H. S.; Hassan, R. Y. A.; Mulchandani, A. Electrochemical Impedance Spectroscopy (EIS): Principles, Construction, and Biosensing Applications. *Sensors (Basel, Switzerland)* 2021, *21* (19), 6578. https://doi.org/10.3390/s21196578.

[62] Ahmed, R.; Nabi, G.; Ali, F.; Naseem, F.; Isa Khan, M.; Iqbal, T.; Tanveer, M.; Qurat-ul-Aain; Ali, W.; Shahzad Arshad, N.; Naseem, A.; Maraj, M.; Shakil, M. Controlled Growth of Mo-Doped NiO Nanowires with Enhanced Electrochemical Performance for Supercapacitor Applications. *Materials Science and Engineering: B* 2022, *284*, 115881. https://doi.org/10.1016/j.mseb.2022.115881.

CURRICULUM VITA

Cristina Gonzalez is a first-generation university student. She received her Bachelor of Science in Mechanical Engineering from the University of Texas at El Paso in 2021. In that same year she continued her education to pursue a Master degree in Mechanical Engineering. She is currently a member of the Center for Advanced Material Research (CMR) team.

Contact Information: gcristina26@yahoo.com

This thesis was typed by Cristina Gonzalez